NUMERICAL AND EXPERIMENTAL ANALYSIS OF KSF LED PACKAGES IN A 65” ULTRA-THIN LED TV

A Thesis

by

Metehan Elibol

Submitted to the

Graduate School of Sciences and Engineering
In Partial Fulfillment of the Requirements for
the Degree of

Master of Science

in the
Department of Mechanical Engineering

Özyeğin University
August 2019

NUMERICAL AND EXPERIMENTAL ANALYSIS OF KSF LED PACKAGES IN A 65” ULTRA-THIN LED TV

Approved by:

Professor Mehmet Arık, Advisor,
Department of Mechanical Engineering
Özyeğin University

Assistant Prof. Dr. Polat Şendur,
Department of Mechanical Engineering
Özyeğin University

Assistant Prof. Dr. Mete Budaklı,
Department of Mechanical Engineering
Turkish-German University

Date Approved: 8 August 2019

For my parents

ABSTRACT

Flat panel display technologies have been well developed over the last decade towards high-end products which have slimmer, higher brightness and wider color gamut (WCG) characteristics. These challenges led to a dramatic increase in power consumption and restricting mechanical design by affecting optical components and also limiting the volume for thermal design. At the present time, LED (light-emitting diodes) technology with some unique advantages such as long life time, high energy efficiency and high reliability is the most desirable solution to overcome the challenges in the high-end TV market. LED TV is a type of LCD (liquid crystal display) television and utilizes LEDs at the backlight in place of the conventional CCFLs (cold cathode fluorescent lights).

A number of phosphor concentrations has been proposed for advanced LED TV systems. The LEDs doped with KSF ($K_2SiF_6:Mn^{4+}$) phosphor have made a rapid penetration to the high-end TV market as a solution to meet the requirement of the wider color gamut. However, the light output of the KSF LEDs is approximately 15% lower than conventional LEDs. Hence, high brightness expectation of the TV must be met by increasing the power consumption of the TV. Considering the thermal sensitivity of a typical KSF phosphor with a high power consumption, the key point is to identify the thermal performance of optical and mechanical components with an optimal LED type to design a thermally and optically stable TV system.

This study focuses on investigating thermal and optical effects of the various LEDs doped with KSF in a 65” LED TV with computational thermal models and experimental studies.

The low inner volume and complex geometry of a TV poses crucial challenges to overcome that has been the main focus of this study. Modeling is initiated with geometry idealizations, and an analytical model (1D resistance network) is established to find out the total thermal resistance to obtain the least thermal resistance in the TV system. CFD (computational fluid dynamics) simulations with a commercial software, Ansys Icepak, have been created to determine 3D heat transfer behavior. Furthermore, the LED junction temperature and the temperature distribution on the LCD surface are predicted with computational models. In the experimental study, the validation of thermal models is investigated with thermal measurements and the optical performances of the TV system for various LEDs are determined with optical measurements. Finally, the thermal and the optical performances of different LED chips are compared with each other.

ÖZET

Düz ekran teknolojileri, son on yılda daha ince, daha yüksek parlaklığa sahip ve daha geniş renk gamlı (WCG) yüksek kaliteli ürünlere doğru evrilmektedir. Bu zorlayıcı özellikler, güç tüketiminde dramatik bir yükselmeye sebep olur ve optik komponentleri etkileyerek mekanik tasarıma ve termal tasarıma kısıtlar getirir. Günümüzde, uzun ömür, enerji verimliliği ve yüksek güvenilirlik gibi avantajlara sahip olan LED (ışık yayan diyotlar) teknolojisi, üst düzey TV pazarındaki zorlukların üstesinden gelmek için en cazip çözümdür. LED TV'ler LCD televizyonun bir türüdür ve arka aydınlatma biriminde geleneksel CCFL (floresan lamba) yerine LED'ler kullanılır.

Gelişmiş LED TV sistemleri için çeşitli fosfor konsantirasyonları önerilmektedir. KSF ($K_2SiF_6:Mn^{4+}$) fosfor katkılı LED'ler ise daha geniş renk gamı ihtiyacına karşı bir çözüm olarak üst seviye TV pazarına hızlı bir giriş yapmıştır, fakat KSF katkılı LED'lerin aydınlatma gücü geleneksel LED'lere göre yaklaşık %15 daha düşüktür. Dolayısıyla, TV'nin yüksek parlaklık özelliğini karşılamak için TV'nin güç tüketimini arttırmak gerekmektedir. KSF fosforun termal hassasiyeti ve sebep olduğu yüksek güç tüketimi de dikkate alındığında, belirlenen optimum LED tipleri ile termal ve optik olarak stabil bir televizyon sistemi tasarlamak için optik ve mekanik komponentlerin termal performansını ortaya koymak kritik öneme sahiptir.

Bu çalışmada KSF katkılı LED’lerin bir 65” TV içerisindeki termal ve optik performansının hesaplamalı termal modeller ve deneysel çalışmalar ile araştırılmasına odaklanılmıştır. Bu kapsamda üstesinden gelinmesi gereken zorluklar TV’nin dar iç hacmi ve karmaşık bir geometriye sahip olmasıdır. Modelleme çalışmaları TV geometrisinin basitleştirilmesi ile başlatılmıştır ve sonrasında sistemin toplam termal direncini ve etkin termal direncini bulmak için bir analitik model (bir boyutlu) kurulmuştur. Üç boyutta ısı transfer davranışını belirleyebilmek için ise Ansys Icepak programını kullanarak CFD (hesaplamalı akışkanlar dinamiği) simülasyonu oluşturulmuştur. Bu CFD modeli ile LED’lerin bağlantı noktası sıcaklıkları ve LCD yüzeyindeki sıcaklık dağılımlarının bulunması öngörülmüştür. Deneysel bölümde ise termal ölçümler ile termal modellerin doğrulama çalışmaları araştırılıyor ve optik ölçümler alınarak TV’nin optik performası çeşitli LED’ler için kontrol ediliyor. Son olarak farklı tip LED çiplerinin TV sistemi içerisindeki termal ve optik performansları kıyaslanıyor.

ACKNOWLEDGMENTS

First of all, I would like to express my most sincere gratitude and thanks to my advisor Prof. Dr. Mehmet Arık for his continuous support, guidance and patience through this thesis. I greatly appreciated his advice on my research.

I would like to thank Dr. Şendur and Dr. Budaklı for being on my thesis committee. Special thanks goes to my friend M. Çağlar Özaydın for his help with preparation of some of my experimental studies. Many thanks goes to my colleagues Dr. Karaman and Dr. Lider for their experience and supported me.

Finally, I would like to thank my parents Leyla and Sabri Elibol for their moral support during my thesis studies.

TABLE OF CONTENTS

LIST OF TABLES

LIST OF FIGURES

CHAPTER I

INTRODUCTION

LEDs used in a TV backlight unit (BLU) have many advantages in last decade compared to traditional backlight units based on cold cathode fluorescent (CCFL) due to long-lifetime, durability and high efficiency. These features offer flexibility on making thinner design and reducing power consumption. However, the challenges in the global TV market get harder day by day with drastic expectations by the customers. TV manufacturers have mostly utilized LEDs in recent years in the LCD module having a backlight unit in order to meet the customer demands such as slimmer, wider color gamut and the brighter LED TVs. LCD TVs have maintained a strong market share since 2004 despite the penetration of the rival products such as plasma display TV, OLED TV and quantum dot TV technologies which are seen in Figure 1.

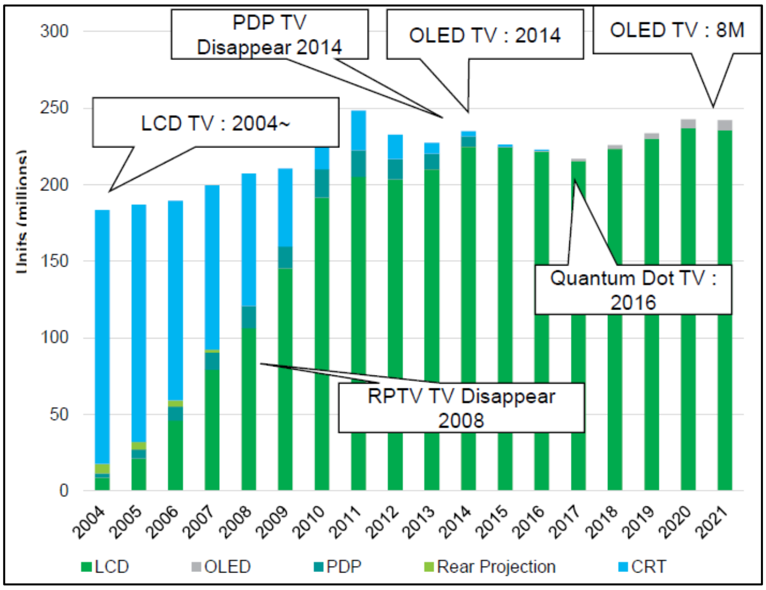

Figure 1: Global TV shipments [1]

The preferred average panel size in the market reached to 43 inch in 2018 and it is expected that the trend will carry on with the larger sized panels over the years [1]. Hence, large size panels, such as 65 inch TVs will be popular in the following years. In 2018, the market share of the TVs 65inch to 85inch was 7%, which can be seen in Figure 2. Most of TV brands moved towards 65" TVs in their product range. Figure 3 shows that large size panels currently take the position in the product range of leader brands as well.

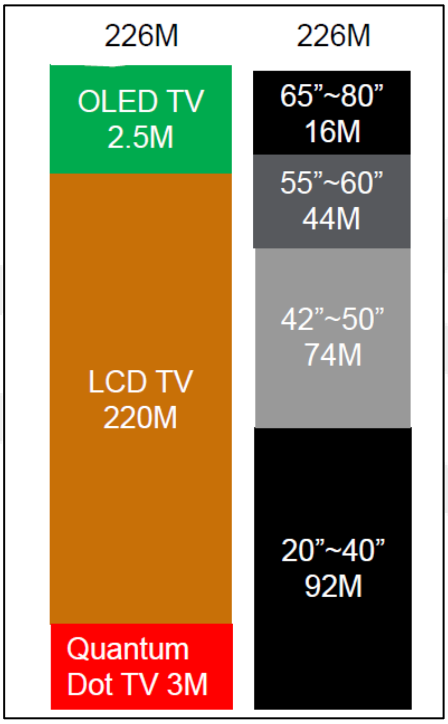

Figure 2: 2018 Global TV technology forecast [1]

The cost is the most significant driving parameter for TV manufacturers. It also depends on the annual forecast of the products. According to Figure 2 and Figure 3, there is a serious demand for large size TVs. It means that the production rate of large size TVs will increase, and the cost is expected to decrease in the future. Thus, TV makers tend to focus on the design solutions of large panels by increasing the optical performance and enhancing the thermal problems.

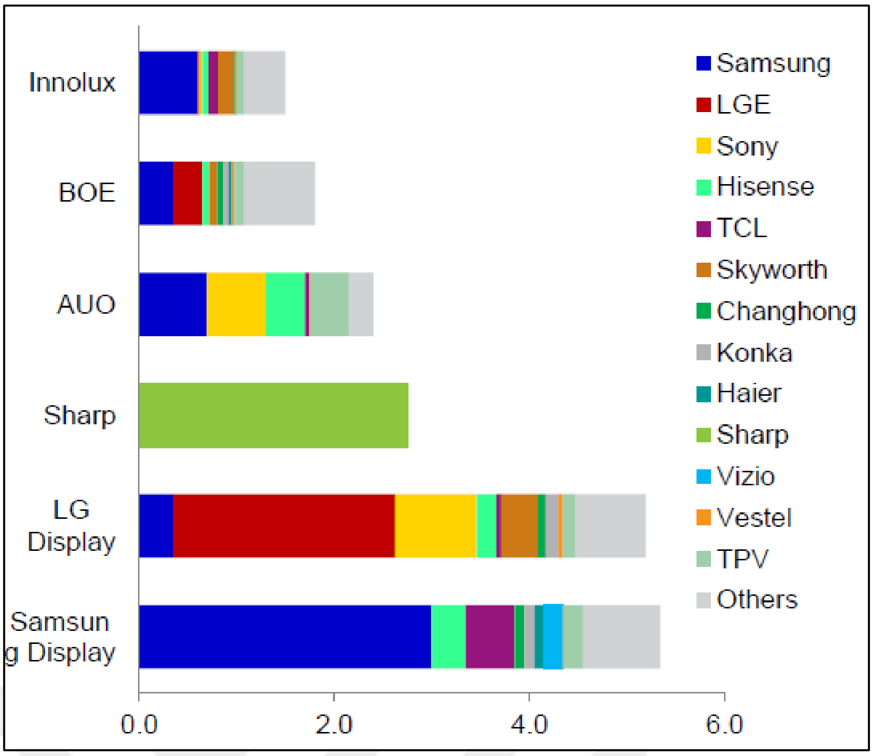

Figure 3: 65-inch LCD TV panel in 2018 by panel maker and target TV maker, million units [1]

With the increase of the panel size, the slim design has also been the trend by the brands dominating the market. However, the slim designs bring about some mechanical constraints which reduce the inner volume of the panels. In this case, the small inner volume affects both optical and thermal designs of the panel. Therefore, TV designers need to optimize both optical and thermal parameters together such as brightness, LED driving current and junction temperature of LED.

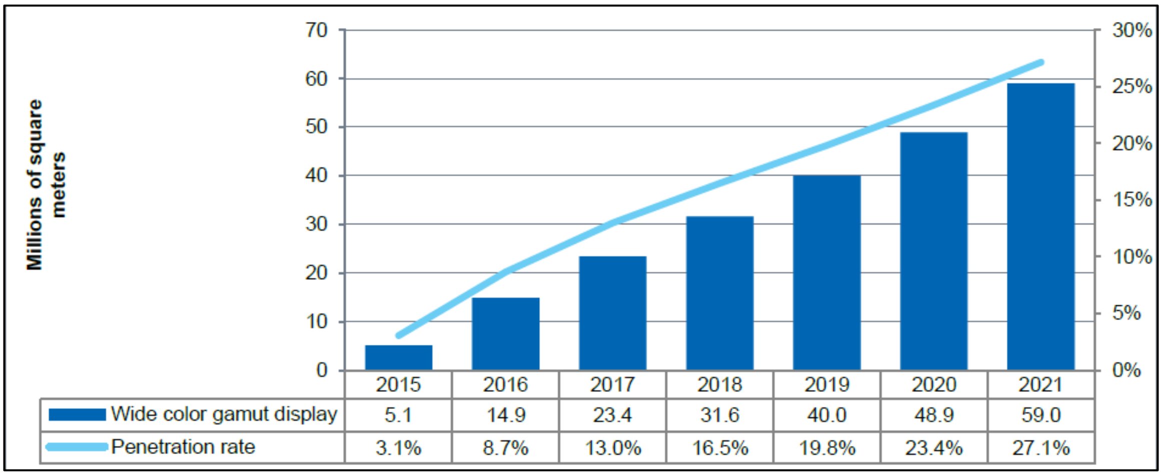

Figure 4: Market forecast for wide color gamut display (unit: area) [2]

The other well-known challenge in the TV market is to meet the requirement of wide color gamut (WCG) which is defined as the coverage area in CIE 1931 color space chromaticity diagram in Figure 5. The color capacity of a TV is expressed with color gamut. The values of the color gamut range from 68% to 72% are comprehended as a standard gamut and the perception of wide color gamut begins with a value of 90% color gamut in CIE 1976. In the TV market, there is an intense competition to reach the WCG. This challenge induces the enlargement of the TV size with WCG, which can be seen in Figure 4. In the present time, there are some solutions in the market to reach WCG feature. TV manufacturers achieve WCG by using quantum dots material without changing main TV system or they prefer OLED TVs, which require high volume investment. However, the most common way at the present market is to utilize the white LED (wLED) doped with $K_2SiF_6:Mn^{4+}$ (KSF) material known as red phosphor.

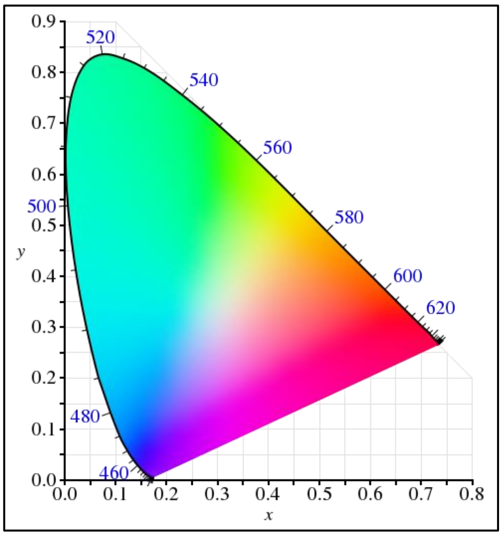

Figure 5: CIE 1931 chromaticity diagram [3]

The standard color gamut in a white LED backlight is provided by using a broadband yellow emitting (YAG) phosphor with a blue LED [4]. However, LEDs with KSF phosphor improve the color gamut amount of 15% in CIE 1976 compared to YAG phosphor [4]. These results show that phosphors with a narrow band emission spectrum such as KSF give the requirement of the wider color gamut in the global TV market and so the color gamut of the TV is particularly dependent on the emission spectrum of the light source used in backlight unit. Beside the WCG advantage, there have been some troubles to use KSF phosphor such as moisture-sensitivity, drop in brightness and the stability against the thermal effects, which regard to the reliability performance. An accelerated damage test given in Figure 6 show the loss of the brightness of KSF phosphors under high blue flux comparing to the YAG phosphor in the long term. According to Figure 6, at least eight times as much as brightness loss has been occurred over time.

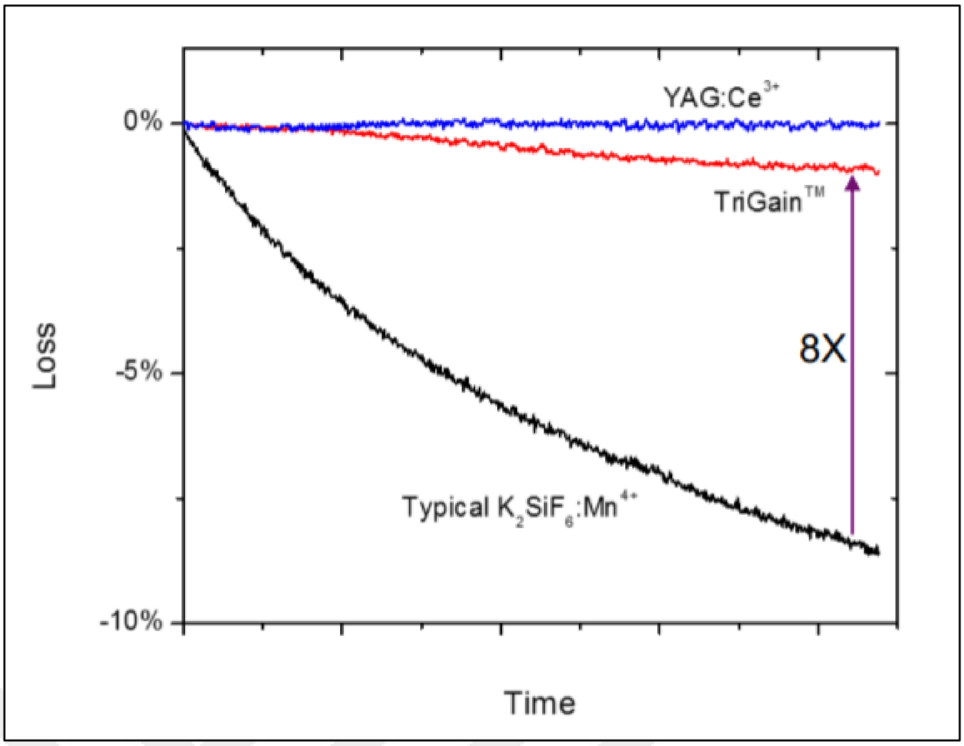

Figure 6: Accelerated light damage test results of YAG, typical $K_2SiF_6:Mn^{4+}$ and TriGain^{TM} (the improved $K_2SiF_6:Mn^{4+}$) under high blue flux [5]

The instant brightness loss can also be seen in Figure 7 for YAG and KSF phosphor emission spectrums under the same level of blue flux. The loss of the brightness is needed to be compensated during the TV system design with two methods. The first one is to increase the input power of the TV system, which causes high LED junction temperature and some thermal effects on LED TV components. With this method, the driving current of a conventional LED including a type of lateral chip in Figure 8 should be optimized by considering the degradation of the luminous efficacy of the LED doped with KSF phosphor.

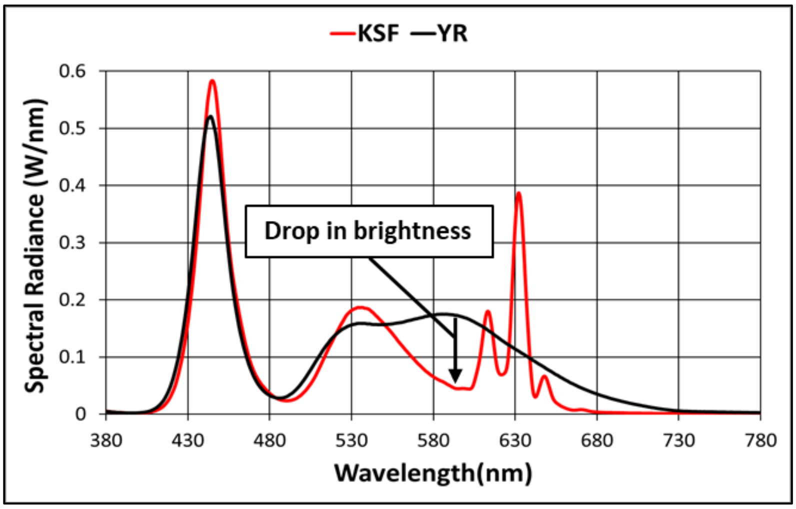

Figure 7: YAG and KSF phosphor emission spectrums exciting with blue LED

The other method is to use LEDs with different design which removes the heat fast from the LED system. These LED chips are made with the process of chip scale packaging (CSP) and called CSP LED in Figure 8. The design of CSP LEDs, which can be seen in Figure 8, have high-level reliability and LEDs can be driven at high current values. The golden wires on CSP LED are not needed because the contact surfaces of LED electrodes are widen owing to the novel design of CSP LED [7]. Therefore, the excess heat is directly transferred to the base of LED chip, which is a distinctive factor comparing to the LED with lateral chip. The other advantage of this design is that there is no need to use a package casing on CSP LED, which can be seen in Figure 8, and it contributes a better luminous efficacy and the reduction of the LED cost. Consequently, a lower thermal resistance (R_{th}) value is expected for CSP LED as well.

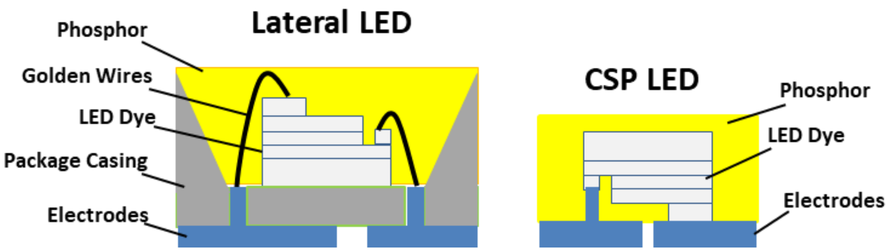

Figure 8: Structures of a typical lateral LED and a CSP LED [6]

1.1 Thesis Objectives

As a result of a detailed market research, it is decided to work on 65” LED TV design with the scope of this study and also to explore how KSF phosphor is crucial to reach WCG target of LED TV. However, it has been a problem regarding to identify an optimal LED type during a LED TV design stage, which the LEDs should provide thermal and optical specifications at the same time such as LED junction maximum temperature and center brightness of TV. Hence, the main purpose of this study is to investigate the thermal and the optical effects of the LED arrays consisting of LEDs doped with KSF phosphor in a 65” LED TV by creating computational thermal models and making an experimental validation study. The complex geometry and the slim design of LED TV are critical to overcome and it is the primary goal of the current study. The main goals of the study are listed as follows;

- Developing an analytical model by creating an idealized thermal resistance network of LED TV to find the LED junction temperatures and understanding the most effective thermal resistance in the system.
- Developing a CFD model to find the LED junction temperature for each LED, determining the temperature distribution on LCD surface and understanding the effect of streamlines inside the plastic back cover over the back metal.

- Validating the simulation values extracted from the thermal models with the results acquired during thermal measurements.
- Controlling the optical specifications of LED TV for each type of LED chip such as lateral and CSP by taking optical measurements.
- Comparing the thermal and the optical performances of lateral and CSP LEDs in a 65” LED TV by considering all the results together.

CHAPTER II

LITERATURE SURVEY

Over the last several decades, there has been a large number of studies regarding to the thermal management of LCD LED TVs. The main purpose of these studies is to understand the heat dissipation on TVs. Thus, it can be possible to design a thinner TV, which has smaller volume to remove the heat from the system with a long lifetime. On the other hand, there are some studies to provide optically better performance on TV by improving the thermal performance with novel cooling methods. Optically, with a brighter and a better color quality LED TV can only be possible in this way. The relevant studies in the literature are hereby summarized as follows.

Chen *et al*. (2008) presented the junction temperature of LED in LCD LED TV by utilizing numerical analysis to define the parameters affecting the LED junction temperature. The numerical simulation is made to calculate the junction temperature for two LED types having different lead frame such as the materials of high strength copper and nickel-iron and validated the simulation results with the thermal measurements. Then, the results led to an improvement more reliable systems [8]. The thermal mura is another issue to be achieved during the TV design stage. The effect is defined as white light leakages on the local regions of LCD surface although the LCD sets on black pattern in Figure 9. Huang *et al*. (2011) argued how to predict the effect of thermal mura on LCD LED TV including edge-lit LED module with an improved simulation method. The method starts trying to find the root cause analysis of thermal mura issue and continue creating CFD simulation with a commercial software (FLOTHERM), but the novelty of this study is that the calculation of thermal analysis is used to build a finite element simulation to find stress distribution on LCD surface, which is the root cause of thermal mura [9].

Figure 9: Thermal mura (corner mura) of 42" LED module [9]

RGB-LEDs in a 37-inch LCD LED TV were also thermally analyzed to see the performance of heat radiation, as well as color uniformity of LCD, developing a thermal simulation in the study of Konno *et al.* (2009). The simulation was performed with and without a heat pipe, the effect of the heat pipe on the heat radiation of RGB-LEDs was investigated by validating the simulation and the measurement results based on LED chip junction temperatures [10]. Tsai and Chen *et al.* (2008) indicated the impact of a high emissive surface treatment on the cooling efficiency of LCD module. They coated the back metal of the module with a high emissive material and CFD commercial software, "Flotherm", was used to see the simulation results of the temperature distributions on LCD surface. The simulation results were compared to the experimental results as well. As the result of the study, cooling was enhanced by the proposed solution in natural convection condition.

Thermal uniformity of LED array on a PCB is one of the key parameters of LED TV thermal design. To meet the parameter, the temperature difference between all LED junction temperatures (T_j) on a PCB is kept close to each other. Yang *et al.* (2009) discussed thermal uniformity in a 13.3-inch LCD LED module by using irregular bracket design without extra thermal cooling device. The thermal enhancement on the thermal uniformity of 54 pieces side view LEDs was observed with an improved CFD simulation built up by a commercial software (FLOTHERM). The thermal uniformity of T_j for the original design and the remove partial area are shown in Figure 10.

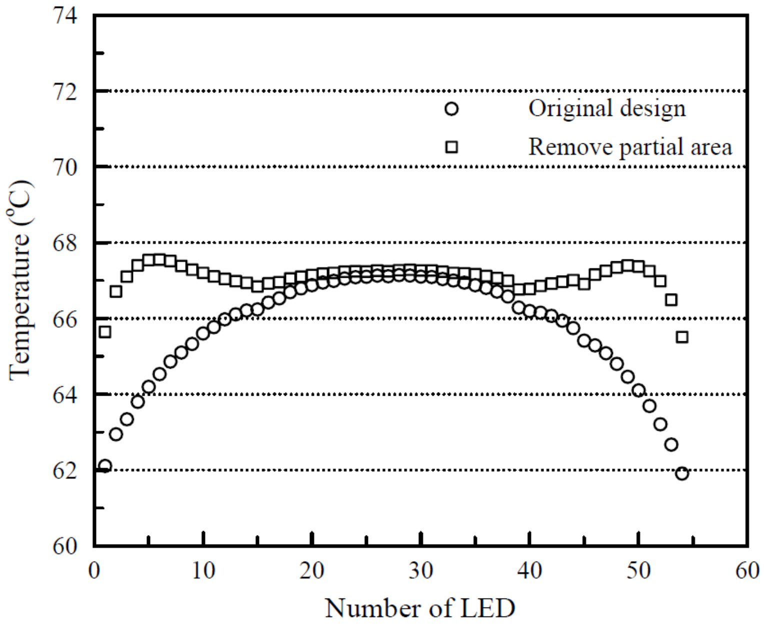

Figure 10: LED Tj curves in thermal simulation compare the original metal bracket with the remove partial area one [12]

The heat dissipation effect of aperture opening on the outer surface of TV module was also examined by Chu and Pan *et al.* (2009). The aim of the study is to provide the improvement of image quality of TV consisting of cold cathode fluorescent lamps (CCFL) backlighting unit, which can be seen in Figure 11. CFD model, which is ANSYS-CFX, was employed in the study only using the right-half portion of the TV module owing to symmetrical shape and boundary conditions. Then, the simulations comprised the analysis of thermal conduction and natural convection were performed with the assumptions of steady state, laminar and incompressible flow. Consequently, opening apertures caused a decrease of the temperature on LCD TV by occurring an effective flow removing the heat from the BLU [13].

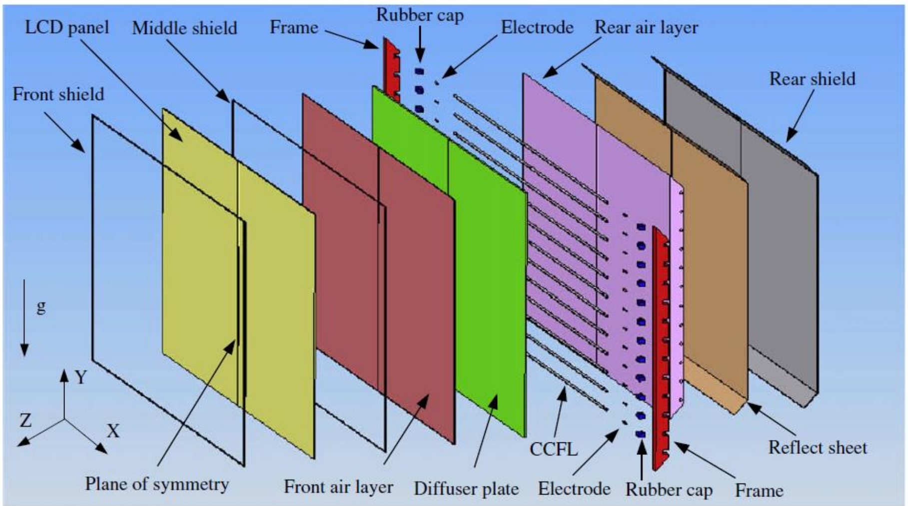

Figure 11: CFD analysis model of a TFT–LCD TV [13]

LED arrays in backlight unit can be assembled to the different side edge of a TV module according to mechanical design constraints, in particular arrays are at two separate side edges in a same TV. Therefore, there are some uncertain issues, such as a long product life time and an adequate image quality on LCD, about thermal management for a LED TV if an array location is at two side edges of a TV. Iz *et al.* (2011) investigated the thermal effects as mentioned above in his study. The study was initiated with a setup of CFD simulation used a commercial software “FloEFD” to predict the temperature distribution of LCD surface, then keeping on with the experimental validation. The results showed that a passive cooling method was sufficient to keep the LED junction temperatures under the maximum operation junction temperature of LEDs [14].

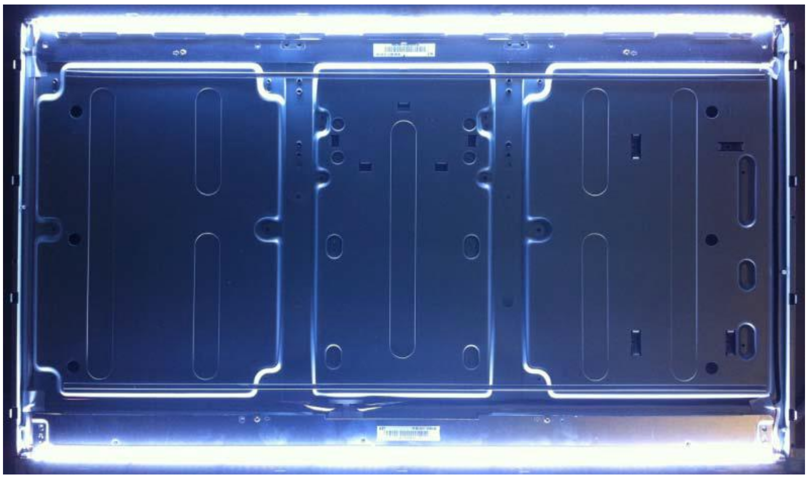

Figure 12: LEDs placement at the top and the bottom side of BLU [14]

In this thesis, the LEDs doped with KSF phosphor in a 65-inch LED TV are examined by using a computational modeling and a thermal network approach to understand thermal and optical effects on TV and decide a correct LED chip type for the TV system. Some assumptions and parameters regarding to the simulations are considered within the scope of this study such as natural convection, incompressible flow and steady-state thermal analysis.

CHAPTER III

LED TV SYSTEM ARCHITECTURE

LED TV system comprises two separate parts that are a backlight unit (BLU) and a liquid crystal display (LCD), which can be seen in Figure 13. Pixels of a LCD are not capable of a light generation so it needs a lighting system. In this instance, the BLU is a lighting unit of LCD and composed of optical and mechanical components as presented in Figure 14. There are two types of BLUs, one of them is a direct type and the other one is edge-lit. These terms are defined according to the LED array position in BLU and determined by technology's concerns as well as benefits.

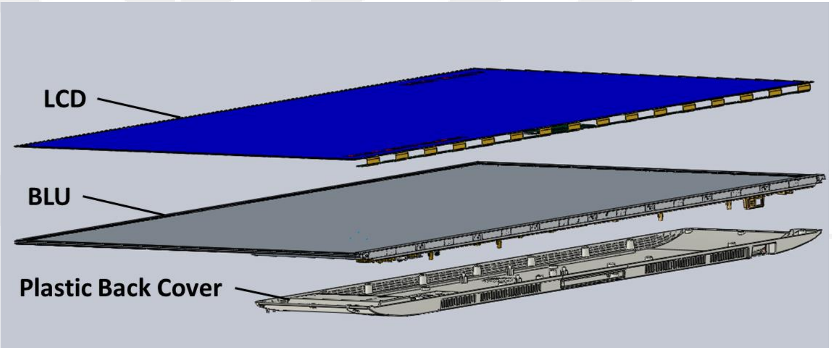

Figure 13: Overall view of 65" LED TV system [6]

In a direct type TV, LEDs are placed on the back metal surface and so the LEDs directly see the LCD. On the other hand, LED placement in an edge-lit BLU is on the edge sides of the panel which cause more thermal issues due to the lower volume for heat dissipation. An edge-lit BLU design in TV market is used to meet thinner TV requirements, which the LED TV within the study includes an edge-lit BLU. Therefore, an edge-lit design needs the usage of different optical and mechanical components. The function of optical components, such as optical films, reflector sheet, LGP (light guide plate) and LED bar consisting of LED array on PCB, inside a BLU is to provide uniform light distribution on LCD surface. Mechanic parts such as Al heat sink, back metal, back metal cover, middle frame and side frame are essential for heat dissipation and system rigidity as well.

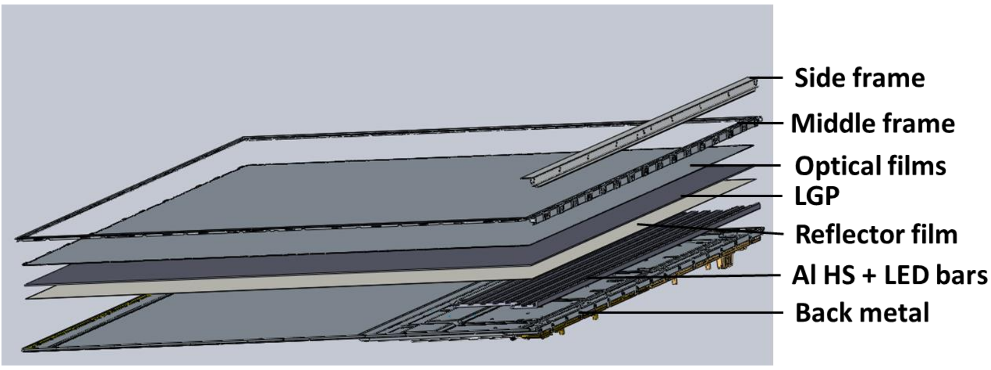

Figure 14: An exploded view of 65-inch BLU [6]

Before thermal issues, the determination of optical targets in Table 1 for 65” LED TV is very critical because the LED TV is primarily an optical system. These targets are defined as depending on the performance of optical components mentioned above. Thermal sensitivity of the optics is a well-known issue, so TV designers need to consider absolute maximum temperature of the components, and keep the optimal temperatures in TV accordingly.

Table 1: Optical targets of 65” ultra slim LED TV

Design parameter	Value
Center luminance for white pattern (Nit)	500
Luminance uniformity for white pattern (%)	80
Color Gamut (%) (NTSC CIE 1976)	90

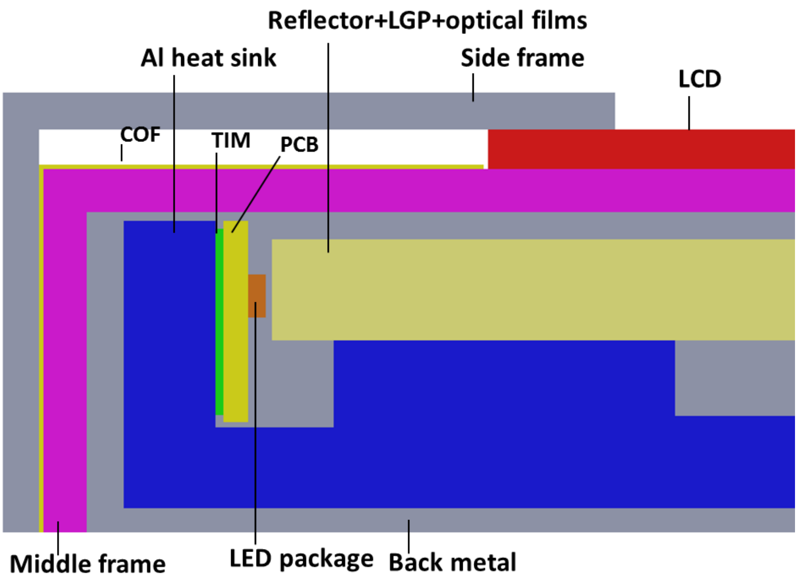

Figure 15: Cross section of a 65" Ultra Slim LED TV [6]

Slim design causes a tight inner structure inside BLU, therefore passive cooling is an only way to remove the heat from the system. Due to the close interaction of components, the convection heat transfer is not effective inside BLU. Hence, the conduction heat transfer is very critical to efficiently dissipate the heat along the system. To understand the tight inner TV structure, the thickness values of the TV components are also presented in Table 2. The total thickness of the ultra-thin TV is about 8.0 mm as well.

Table 2: Critical component thickness [6]

Components	Thickness (mm)
PCB	0.8
TIM	0.25
Al heat sink	3.0
Back metal cover	1.0
Optical components	3.2
Middle frame	1.2
LCD	1.3

3.1 Liquid Crystal Display (LCD)

LCD mainly consists of many layers such as vertical and horizontal light filters, also called as polarizers, glass layers and color filters dividing white light into three primary colors to occur TV content. There are three sub pixels on LCD, named red, green and blue, which can be seen in Figure 16. These pixels are not self-emitting so a BLU provides uniform light distribution along the LCD surface.

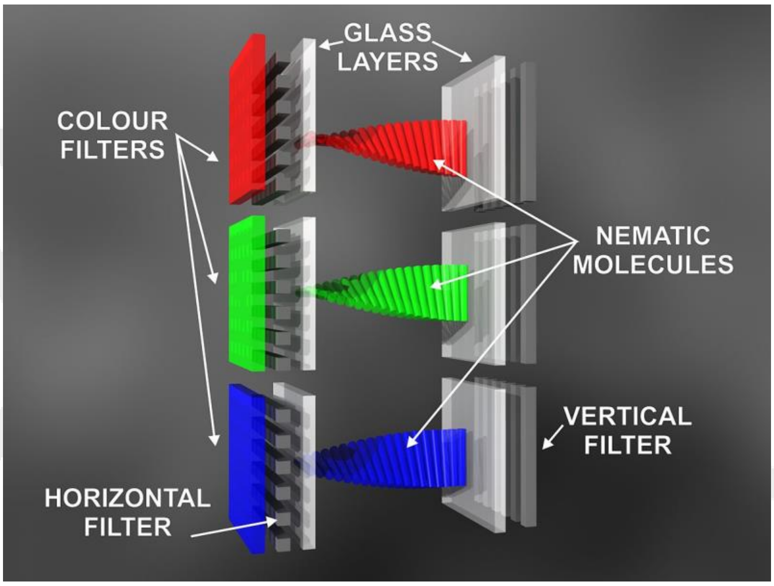

Figure 16: LCD RGB subpixel [14]

To drive a LCD, the connection parts such as a source board and a COF (chip on film) IC (integrated circuit) in Figure 17 are also crucial. These parts generate heat but the heat is neglected within the scope of the study owing to no conduction heat transfer. However, at the end of the design stage the temperatures of the parts need to keep under maximum values in Table 3.

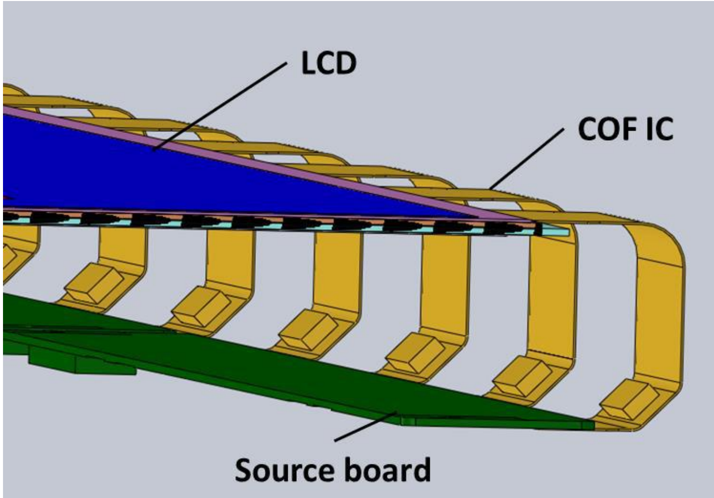

Figure 17: LCD connection parts, COF IC and source board [6]

Table 3: LCD absolute maximum values [6]

Items	Maximum value
LCD surface temperature (˚C)	65
COF IC temperature (˚C)	125

3.2 Backlight Unit Components

3.2.1 LED Bar

LED bars as presented in Figure 18 are the light source of BLU besides being the main heat source in TV, which occurs LED arrays attached to a PCB (printed circuit board) by surface mount technology. PCB is made of Al material, called metal core PCB (MPCB), to increase the thermal conductivity. There are also copper lines on PCB to provide electrical conduction as well. The top layer of PCB is covered by a di-electric insulator.

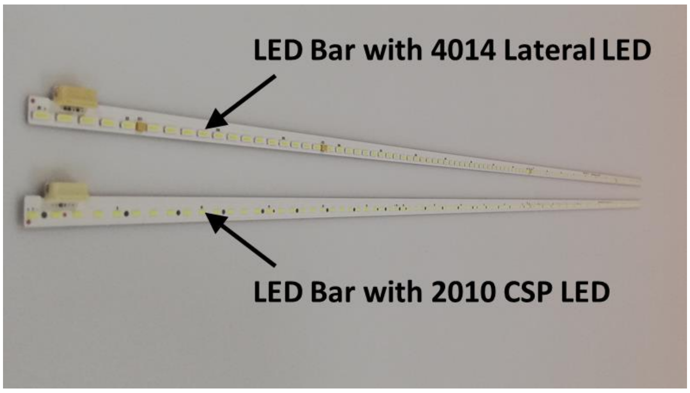

Figure 18: LED bars with Lateral and CSP LEDs

LEDs are lined up along PCB by using surface mount method. In this study, there are two types LEDs. The first one is to have lateral chip technology, the other one is to have CSP chip technology.

3.2.1.1 LED Packages

The total power consumption of a TV highly depends on the efficacy of the light source. Therefore, high efficiency LEDs are used for the optical design of TV to obtain lower power consumption and higher brightness targets. Thermal performance of the light source is mostly the key point to provide minimum lifetime for 30.000 hours at operating condition. As mentioned in the previous section, to reach wide color gamut requirements of TV, the LEDs with KSF phosphor should be utilized. However, the KSF phosphors show a particular sensitivity to high temperature. Hence, the selection of optimal LED type is a big challenge during the design stage as well. 4014 (4.0x1.4x0.7mm) lateral LEDs and 2010 (2.0x1.0x0.35mm) CSP LED, which are mid-power LEDs, are separately investigated within the study.

3.2.1.1.1 Lateral LED

Lateral LEDs, which is the conventional LED, are the most common LED used in TV market due to high production rate. They consist of the parts of LED dye, package casing, electrodes, phosphor and golden wires, which provide a connection between electrodes and p-n junctions, in Figure 19. There are some disadvantages of Lateral LED design but a major one is a poor heat dissipation performance. Furthermore, golden wires are too sensitive against thermal and mechanical effects so it causes local hotspots on LED [16]. The specifications of Lateral LED are presented in Table 4. 288 pieces 4014 lateral LEDs have been lined up on PCB to reach the optical targets of TV within the study.

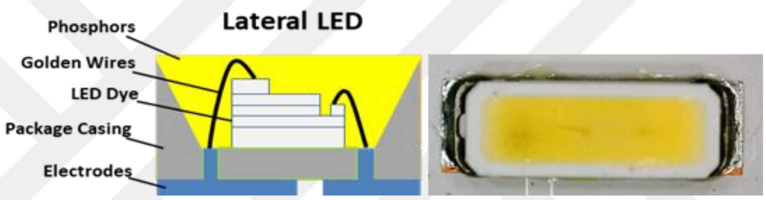

Figure 19: Schematic of a lateral LED [6]

3.2.1.1.2 CSP LED

CSP LEDs are a breakthrough technology and start to dominate the market. As illustrated in Figure 20 there are no package case and golden wire in the design, and LED dye is directly mounted on PCB by SMT (surface mount technology). The LED is totally covered by solidified encapsulated silica gel mixed with KSF phosphor [16]. Hence, CSP LEDs with better heat dissipation and higher light output have stood out in the market. CSP LED characteristics can be seen in Table 4. There are two significant regions used for the two different thermal resistance (R_{th}) of CSP LEDs. One is junction to solder and the other is 3mm away from the junction. In this study, R_{th} for junction to solder is used for thermal simulation and the R_{th} for 3mm away from the junction is for thermal measurements. CSP LED structure is given in Figure 20. 264 pieces of 2010 CSP LEDs have been lined up on the PCB to meet the optical requirements of TV within the study.

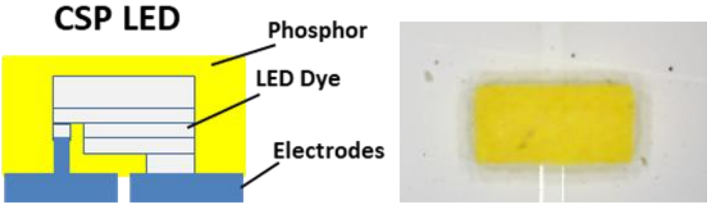

Figure 20: Schema of a CSP LED [6]

Table 4: 4014 lateral and 2010 CSP LED specifications [6]

Items	4014 Lateral LED	2010 CSP LED	Unit
Forward voltage	5.9	3.0	V
Forward current	81	175	mA
Max. forward current	120	500	mA
R_{th} (junction to solder)	25	2	K/W
R_{th} (3mm away from junction)	-	13	K/W
T_{j-max} (˚C)	110	145	˚C
$T_{j-max-operation}$ (˚C)	88	116	˚C

3.2.2 Thermal Interface Material (TIM)

To obtain an optimal heat transfer between LED bar and heat sink, a good interconnection among surfaces is essential. A thermal tape as TIM is used for the study to attach LED bar to heat sink. To provide uniform heat dissipation along the LED bar, some concerns need to be eliminated such as clean surface, adequate thermal conductivity and excellent adhesion. Local overheating on the LED bar arises due to the air gaps between LED bar and heat sink if the LED bar is not taped to heat sink very well.

3.2.3 Heat Sink (HS)

As mentioned in the previous sections, the passive cooling method is the most conventional option to remove the heat from the system due to low inner volume in BLU. Hence, the primary cooler in BLU is a heat sink in Figure 21, namely aluminum bracket, made up of an aluminum material. Aluminum materials with light weight and high thermal conductivity, which is 177 W/m-K, have favored in the production of heatsinks. The heat sink is assembled to a metal back cover with screws instead of thermal bands, which cause poor surface contact and needed an additional labor in a production line.

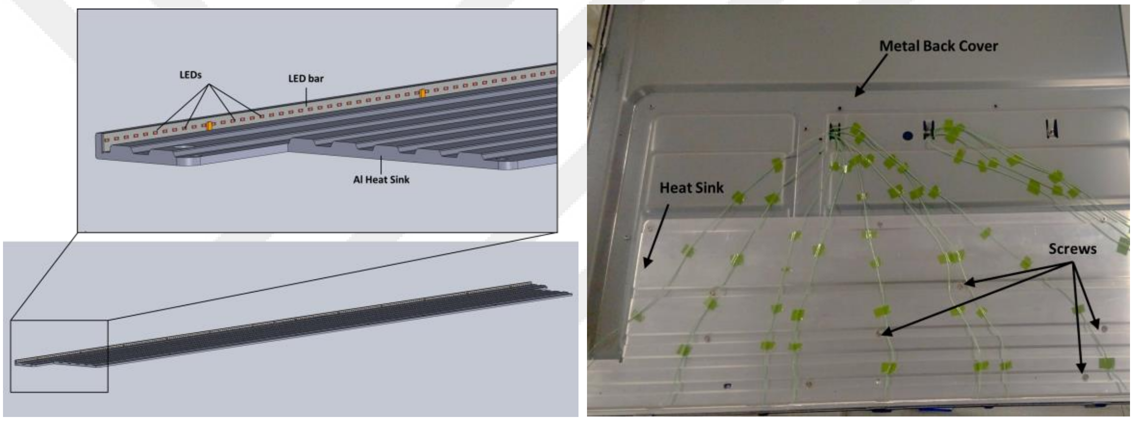

Figure 21: Aluminum heat sink with a LED bar [6]

3.2.4 Metal Back Cover (Metal BC)

Metal back cover is a main housing of mechanical and optical components as presented in Figure 22. It is made of galvanized sheet metal. There are important advantages of galvanization process. The major one is to avoid premature rust and corrosion, which provide long lifetime to the metal [17]. Besides that the benefits, the process is lower cost than stainless and remarkable resistance to mechanical damages. The dipping galvanization process (SGCC) is also applied to the back metal within the study instead of electro galvanization (SECC). Lastly, the metal back cover is second passive cooler after Al heat sink in the system due to high thermal conductivity, which is 41.5 W/m-K.

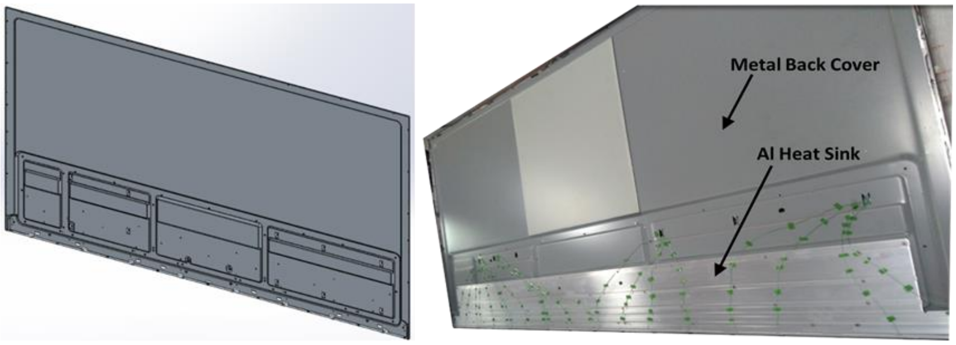

Figure 22: Metal back cover [6]

3.2.5 Reflector Sheet

The placement of reflector sheet, which represented in Figure 23, is on the inner surface of the metal back cover. It is an optical component which provides the light regain by redirecting the light escaping the system with the high reflection rate. The reflector sheet contributes a uniform light diffusion along the LCD as well as the increase of optical efficiency. The material of the sheet is PET (polyethylene terephthalate) and the typical thickness is 0.4mm. Besides a number of optical advantages, it offers poor thermal conductivity in BLU.

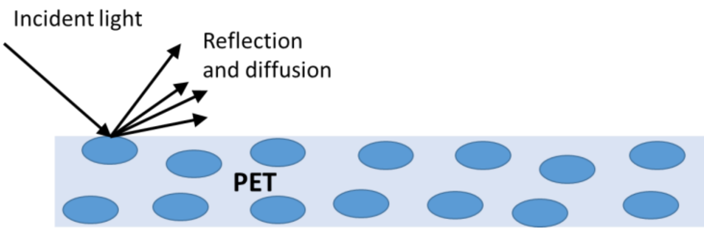

Figure 23: The schema of reflector sheet [21]

3.2.6 Light Guide Plate (LGP)

The emitting light from the LEDS at the edge side of BLU should be uniformly directed towards the LCD. The patterned LGP make the light direct to the active screen with the effects of reflection, refraction and total internal reflection (TIR). The working principle of LGPs can be generally represented in Figure 24. There is a pattern on the LGP back surface and it provides uniform light distribution along the LCD. The pattern are printed on the back surface of LGP with different manufacturing process such as ink printing, hot roll stamping and laser engraving. LGPs are generally made of PMMA (poly methyl methacrylate) material and have a low thermal conductivity. Additionally, thermal sensitivity of LGPs is very high so the structural deformation can be easily seen on it.

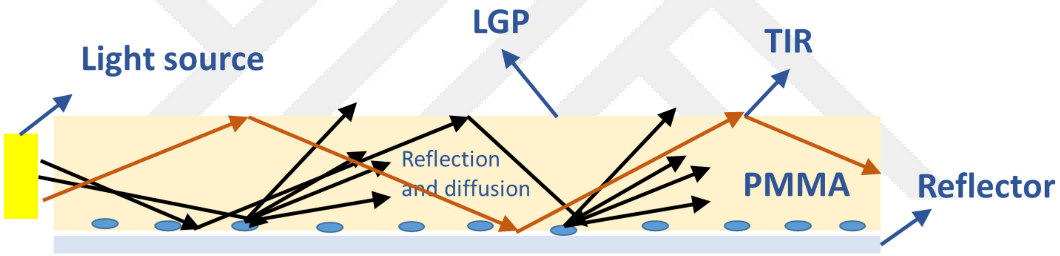

Figure 24: Behavior of light inside the LGP [18]

3.2.7 Diffuser Sheet (DS)

The function of diffuser sheet is to uniformly distribute the incident light from LGP throughout the LCD. The rough material of DS is PET which used as substrate and the top surface of DS is coated by acrylic beads as illustrated in Figure 25 to enhance the light diffusion as well as a low concentration beads on the bottom surface to prevent the electrostatic discharge (ESD) with other components. Two diffuser sheets are utilized in BLU structure. One is mounted on the LGP and the other one is placed after prism on prism sheet.

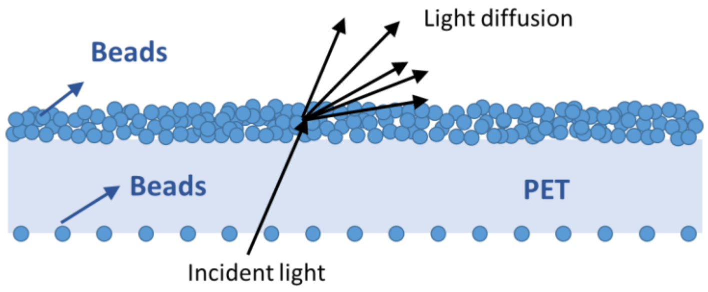

Figure 25: The schematic of a diffuser sheet [20]

3.2.8 Prism on Prism Sheet (POP)

The sheet consists of two prismatic structures laminated each other by vertical and horizontal prismatic sheets. The aim is to collimate the incident light at the center of the LCD to increase the brightness, which can be seen in Figure 26. PET is used as the substrate material. The thermal expansion due to thermal issue causes the sheet undulation on POP because of the lamination process. The placements of POP and the other optics are presented in Figure 27.

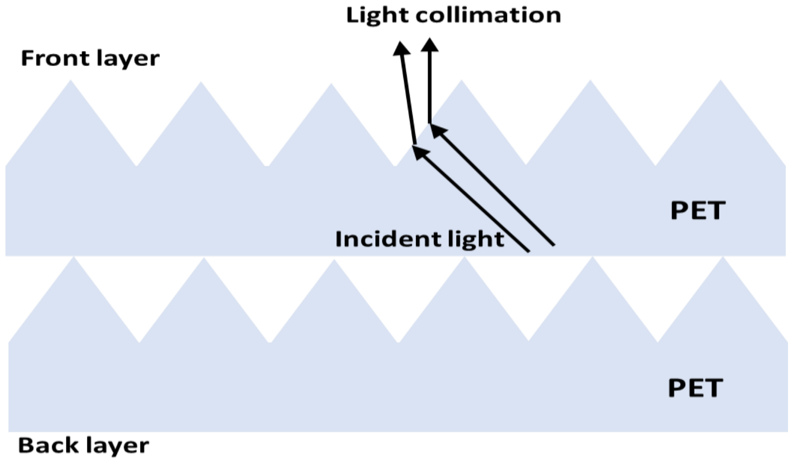

Figure 26: The structure of a POP sheet [19]

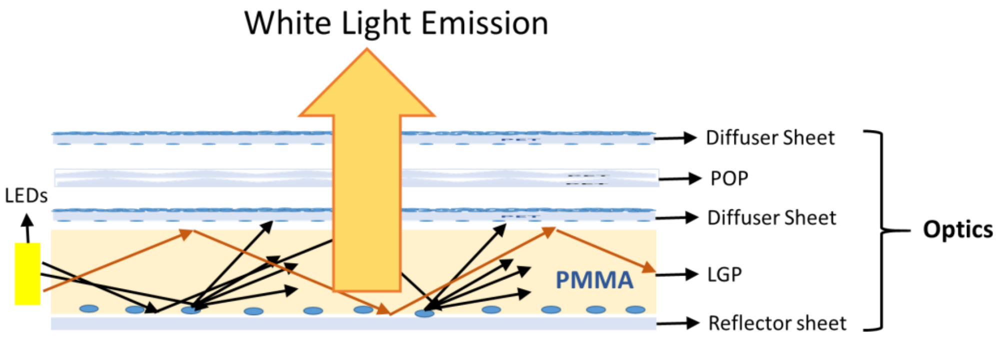

Figure 27: The optical structure of edge-lit BLU [18]

3.2.9 Middle Frame (MF)

Middle frame keeps the BLU optics inside the metal back cover and contributes immobility of the optics by considering the sensitivity against the mechanical effects. MF is made of plastic material and assembled to metal BC. There is two side tape on the top of MF to safely mount the LCD. The LCD is taped on MF with the tape as well. The plastic injection process is utilized to produce the MF.

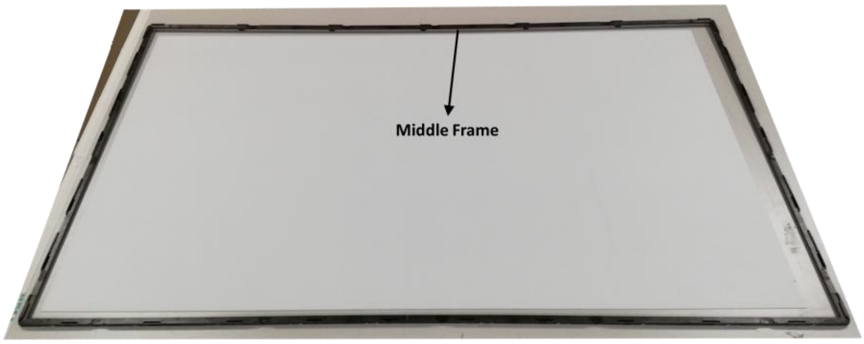

Figure 28: Middle frame

3.2.10 Plastic Back Cover (Plastic BC)

The plastic back cover is assembled to the back side of metal back cover and so a closed volume between the back side of metal and the plastic back cover is created. The occurrence of various flow regimes in the volume are expected during the study and also the grid structure on the plastic back cover can be effective to remove the heat generation on the surface of the metal back cover. However, the complex geometry of the plastic back cover needs to be achieved during the simulations. The plastic back cover is designed to cover about the half of the back metal due to the aesthetic concerns.

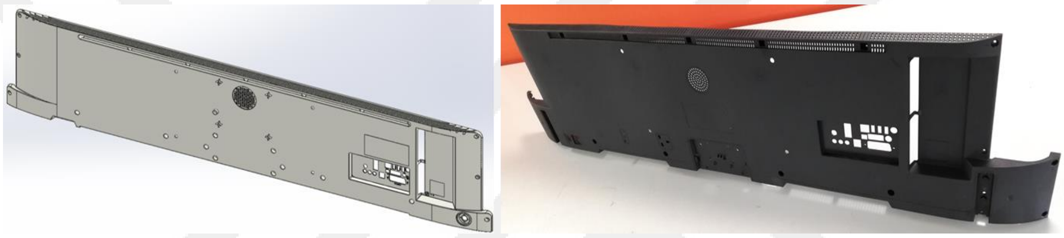

Figure 29: Plastic back cover [6]

3.2.11 Side Frame

Side frame is made of an aluminum material and assembled to the metal BC with screws. The purpose of the side frame is to keep the bottom edge of the LCD instead of well taping the LCD on the MF. However, the main function is regarding to the aesthetic. Hence, there is no effects on thermal and optical performance of LED TV.

CHAPTER IV

COMPUTATIONAL STUDY

Thermal models have been improved to find out the limitations of a system at maximum condition and to optimize system parameters such as driving current, power consumption, junction temperatures and total light output. Thus, the models provide a prediction about the parameters in a simulation domain. The most important parameter in a LED TV system is the junction temperature of LEDs as well. The deformation or the permanent damages on the components of the TV can be seen even if the junction temperature exceeds the absolute maximum ratings. Additionally, the lumen output degradation of LEDs is also occurred in time. The junction temperature is highly correlated to the lifetime of the product and lumen output efficiency of LEDS. Therefore, the maximum permissible temperature should be defined for LEDs in a TV before prototyping in the design stage. Otherwise, the conventional methods such as trial and error cause time-consuming and higher costs, which exponentially increase with extending the size of TVs. In this case, thermal models with saving time and costs have favored in a LED TV market.

In this thesis, an analytical (1D resistance network) and a CFD models have been created to predict the junction temperatures of both lateral and CSP LEDs doped with KSF phosphors and then the experimental validation studies have been made to reach more accurate simulation results. Before starting the modeling, the simplification operations on the mechanical structure are made due to the complex geometry of the TV to save the simulation time and generate a conformal mesh structure for the CFD simulation. Hence, the complex geometry were converted to the prismatic objects such as the shapes of square and rectangular as illustrated in Figure 30.

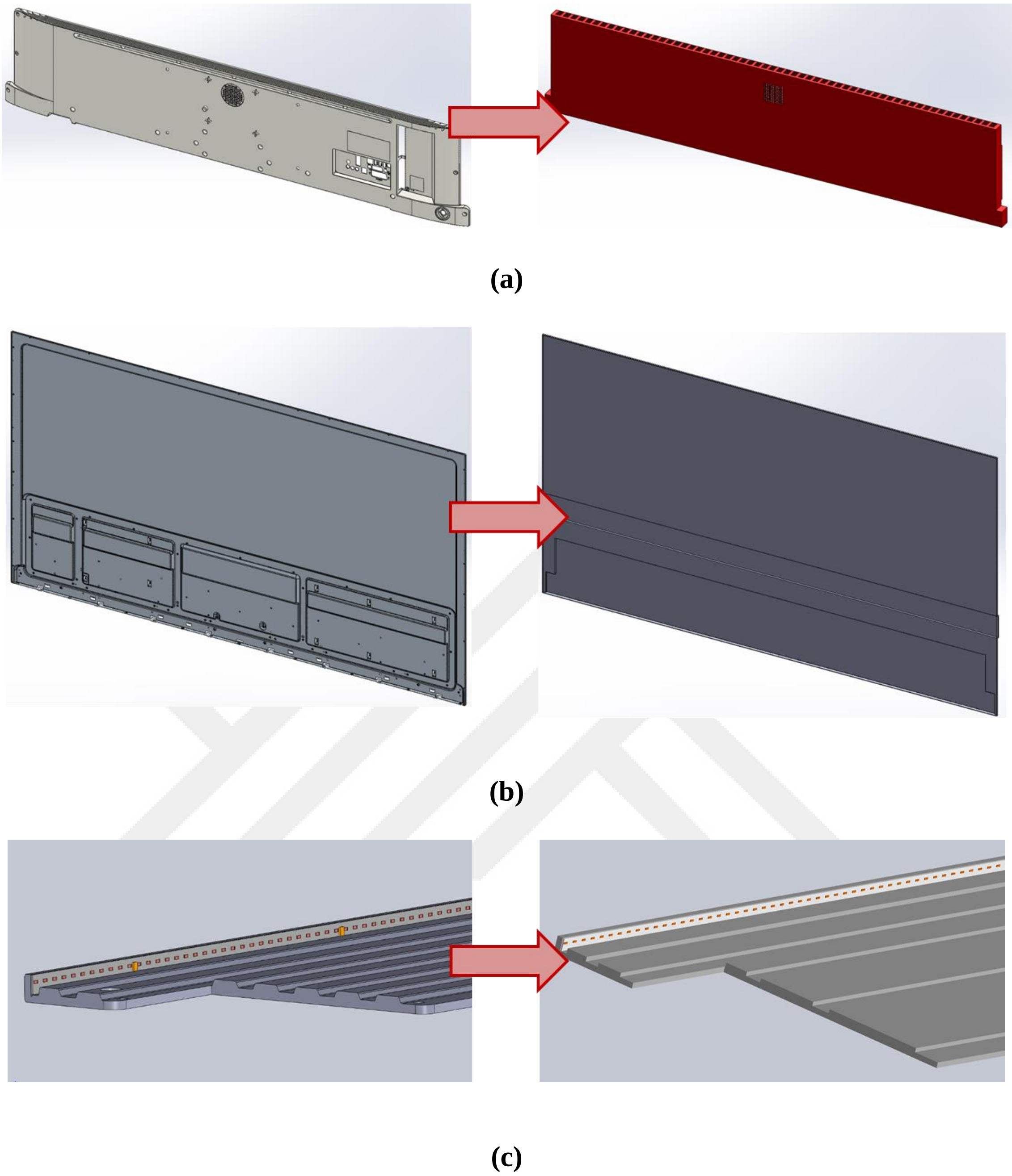

Figure 30: Idealized geometries of (a) plastic BC, (b) metal BC and (c) heat sink [6]

Within the mechanical simplification, the geometries such as holes, rounded, chamfers and circular shapes were removed but the main structure affecting the heat dissipation were preserved in the system. Additionally, the optical components except LED bars such as reflector sheet, LGP, diffuser sheets and POP were geometrically combined as an all in one structure called the optics, which can be seen in Figure 27. The thermal conductivities of the optics were assumed the same since the rough materials of the optics were quite similar to each other. As a result, thermal models in the following sections were occurred based on the mechanical simplifications.

4.1 Analytical Modeling

An idealized thermal resistance network within the studies of the analytical modeling is created by considering the heat transfer path, which is an assumption, between LED to the ambient in Figure 31. There are two surfaces, which are the sides of LCD and metal BC, to quit the system for the heat when looking at the Figure 31. The heat generation from LEDs is removed from the system by conduction and convection heat transfers as well. Therefore, two different heat transfer coefficients (h_{conv}) for the surfaces of LCD and metal BC need to be calculated to reach the thermal resistance values (R_{conv}) of convection heat transfer.

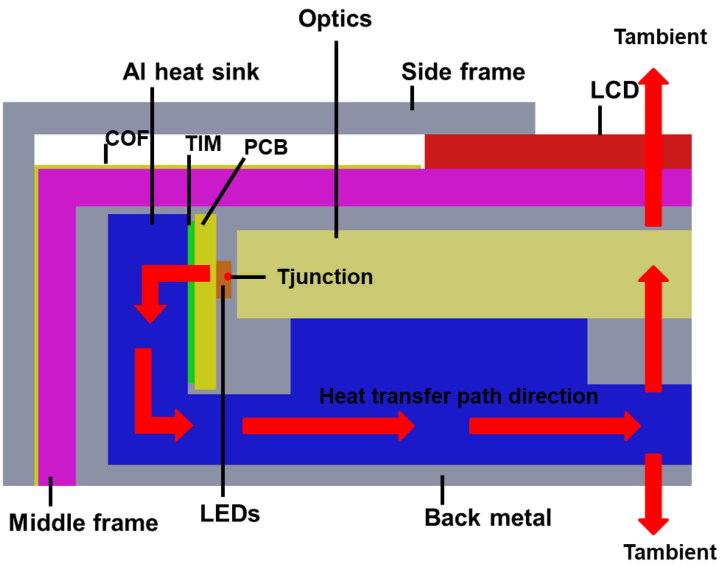

Figure 31: Cross sectional view of heat transfer path in one dimension [6]

In this case, Equation 1 is utilized to find the coefficients and then the heat flux values are extracted from the CFD results as well as the downstream temperature (T_d). Then, R_{conv} can be calculated by Equation 2 for both surfaces, which A_s is the surface area.

$$h_{conv} = q/(T_d - T_{ambient}) \tag{1}$$

After finding the thermal resistance of the heat transfer coefficient, thermal resistance values in Figure 32 for each component are computed by Equation 3 by assuming all LEDs in parallel each other. Thermal conductivity (k) and the surface areas of the components are also presented in Table 5.

$$R_{conv} = \frac{1}{h_{conv} A_s} \tag{2}$$

The idealized model is executed to calculate the junction temperature of LED at 40 °C ambient temperature (T_a) with 112W heat power ($P_{thermal}$), which assumed for a 20% the light conversion efficiency with Equation 4. The calculated thermal resistance within the idealized model are presented in Table 5. The results show the junction temperatures of 4014 lateral LEDs and 2010 CSP LEDs are 84.2 °C and 75.3 °C, respectively. In the chapter regarding to experiments, the validation is made for the simulated junction temperatures.

$$R_{th} = \frac{L}{kA} \tag{3}$$

$$T_{junction} = T_a + R_{th\_sum} . P_{thermal} \tag{4}$$

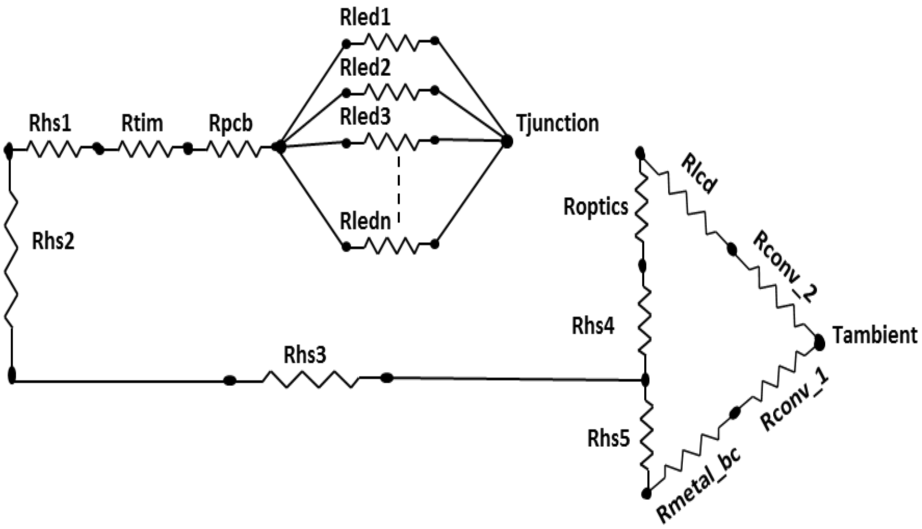

Figure 32: Idealized thermal resistance network for 65" LED TV [6]

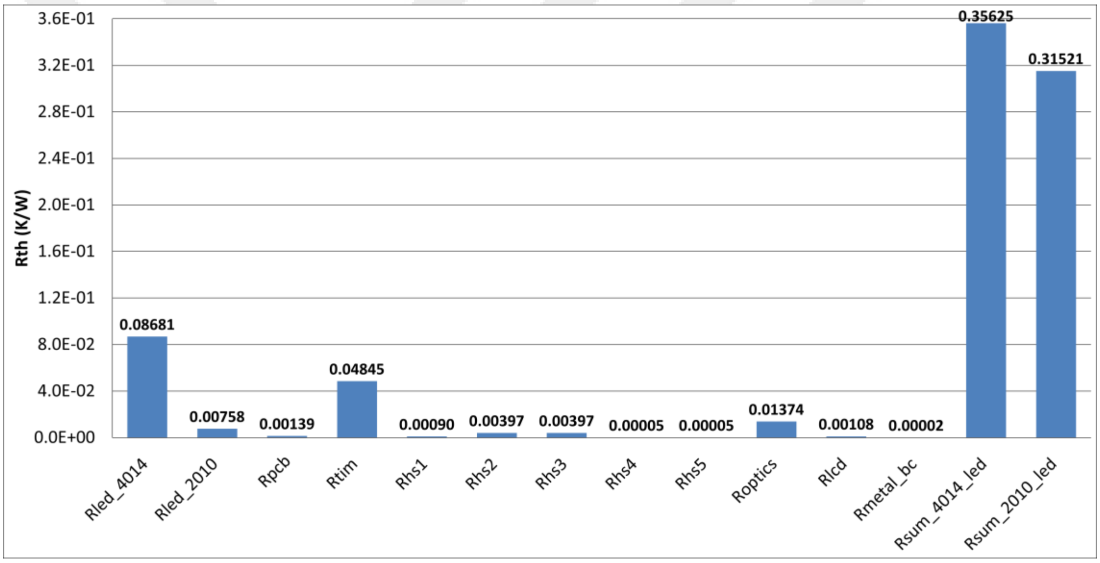

Figure 33: Individual thermal resistances [6]

To understand the effectivity of each resistance in the system, the individual thermal resistances in Figure 33 are calculated. According to the Figure, the resistances of 4014 lateral LED seem highest. It means that there is a significant resistance against the heat transfer of the junction to PCB so high junction temperatures can be expected for the case of 4014 LEDs because the heat cannot be removed the system in adequate time. The other component having high resistance is the thermal tape (TIM), which provides the attachment LED bar to heat sink. TIM is very close to the main heat source so it is a critical component to efficiently conduct the heat to the heat sink.

Table 5: The conductivities and the thermal resistances in the analytical model

Thermal Resistance	**Conductivity (W/m-K)**	**Thickness (mm)**	**Area (mm^2)**	**R_{th} (K/W)**
$R_{LED\ 4014}$	-	-	-	25
$R_{LED\ 2010}$	-	-	-	2
R_{pcb}	61.5	0.80	$9.38x10^3$	$1.39x10^{-3}$
R_{tim}	0.6	0.25	$8.60x10^3$	$4.84\ x10^{-2}$
R_{hs1}	177.0	1.50	$9.38\ x10^3$	$9.03\ x10^{-4}$
R_{hs2}	177.0	3.00	$4.27\ x10^3$	$3.97\ x10^{-3}$
R_{hs3}	177.0	2.00	$2.84\ x10^3$	$3.97\ x10^{-3}$
R_{hs4}	177.0	2.00	$2.28\ x10^5$	$4.95\ x10^{-5}$
R_{hs5}	177.0	2.00	$2.28\ x10^5$	$4.95\ x10^{-5}$
R_{metal_BC}	41.5	1.00	$1.24\ x10^6$	$1.95\ x10^{-5}$
R_{optics}	0.2	3.30	$1.20\ x10^6$	$1.37\ x10^{-2}$
R_{cell}	1.0	1.30	$1.21\ x10^6$	$1.08\ x10^{-3}$
R_{conv_1} (Metal BC)	-	-	-	$3.92\ x10^{-1}$
R_{conv_2} (LCD)	-	-	-	$6.67\ x10^{-1}$

4.2 CFD Modeling

Computational methods is utilized to predict a behavior of fluid flows and heat in a relevant system. CFD combines various disciplines, which are physics, mathematics and software engineering, in a same domain to create comprehensible models as well. Industry prefers CFD models to decrease the cost of some experiments and perform impossible experiment in a real life. Of course, there are many more areas for the usage of the models such as weather prediction in meteorology, device cooling in electronics and aerodynamic design in aerospace industry. In the study, the LED junction temperatures, the temperature distribution along the LCD and the flows inside the plastic

BC are investigated by building a CFD model with a commercial software, Ansys Icepack, in which the simulation domain occurring for the study is given in Figure 34.

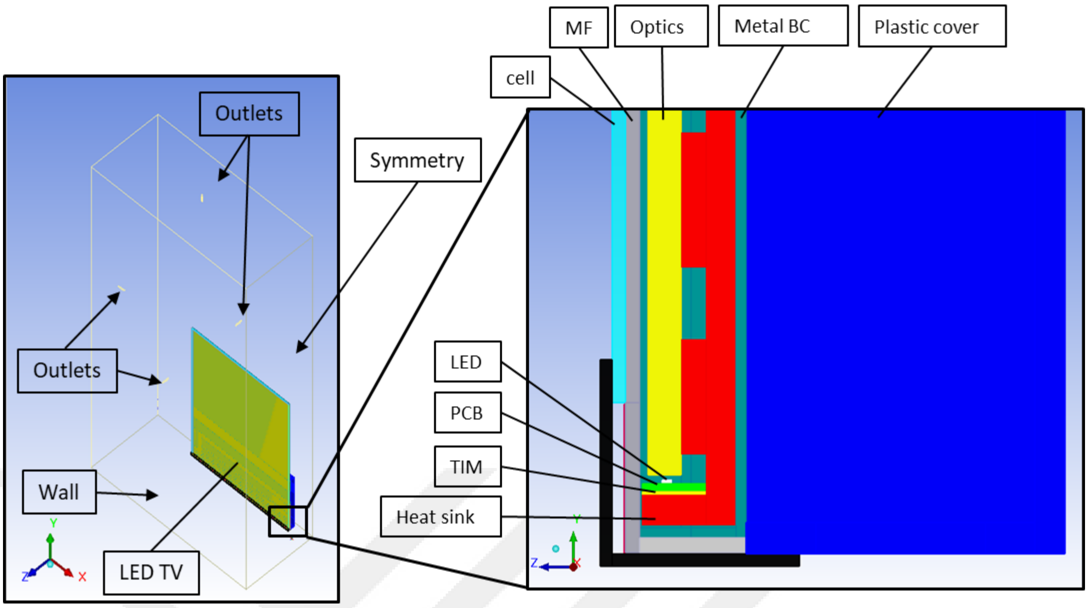

Figure 34: CFD simulation domain

Before establishing a simulation domain, some assumptions are made to save the time and reaching conformal mesh structure. The first one is to use simplified mechanics and creating the models with prismatic objects, which give more accurate results. The second one is to assume perfect interconnection between the objects to get easier mesh generation. Finally, the left and right sides of the LED TV is fully symmetrical to each other because there is no difference of mechanical and boundary conditions for two sides. Thus, the only half side of TV is imported to the simulation domain.

4.2.1 Simulation Domain

The half part of simplified geometry is directly imported to the simulation domain. The geometry is covered with a cabinet which is a kind of simulation environment occurred the wall conditions such as outlet, wall and symmetry. The bottom plane of the geometry is defined as a wall condition meaning that there is no mass and energy transfer. The symmetry side is limited as the feature of a symmetry wall condition meaning there is zero heat flux condition at the symmetry plane. The other planes are expressed as an outlet condition making possible the mass and the energy transfer in the plane. The final domain is presented in Figure 34.

4.2.2 Material Properties

Total input of typical electrical power of the LEDs in the system is 140W but the light conversion efficiency is accepted as 20% so the total heat power in the system should be 112W. The total heat power is divided among the individual LED, thus 0.39W for lateral LED and 0.424W for CSP LED is set for the simulation input as illustrated in Figure 35.

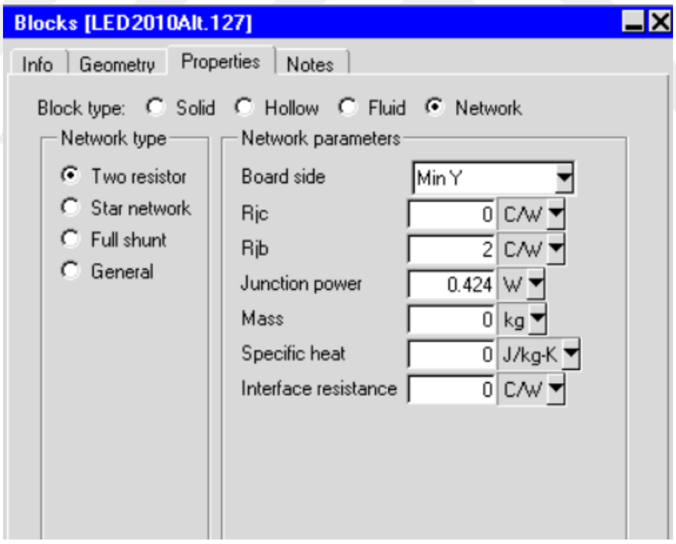

Figure 35: Power and resistance inputs for CSP LED

There is an assumption of the conduction heat transfer in the system, so the thermal conductivities of the other components in Table 6 are separately inserted by the property window in Figure 36.

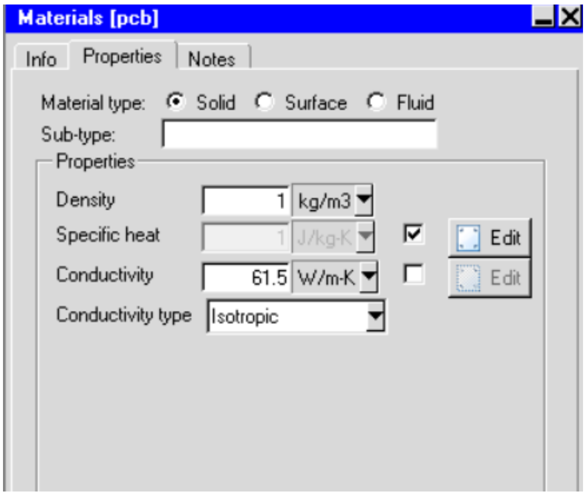

Figure 36: Properties Tab for PCB conductivity input

Table 6: Material conductivities and resistances [6]

Materials	k (W/m-K)	R_{th} (K/W)
4014 Lateral LED	-	25
2010 CSP LED	-	2
PCB	61.5	-
TIM	0.6	-
Al heat sink	177	-
Back metal	41.5	-
Middle Frame	0.2	-
Optics	0.2	-
LCD	1.0	-

4.2.3 Mesh Sensitivity Study

Mesh generation is a critical section for CFD simulations since the finite volume analysis is used for the calculations during the simulation. Hence, the computation of the finite volume analysis is forced to associate with the nodes to each other if there is the high number of elements in a mesh. Therefore, the accuracy of the simulation extremely decrease or the simulation is failed. To avoid the meshing problem and save the time, mesh sensitivity study is made to optimize the number of elements.

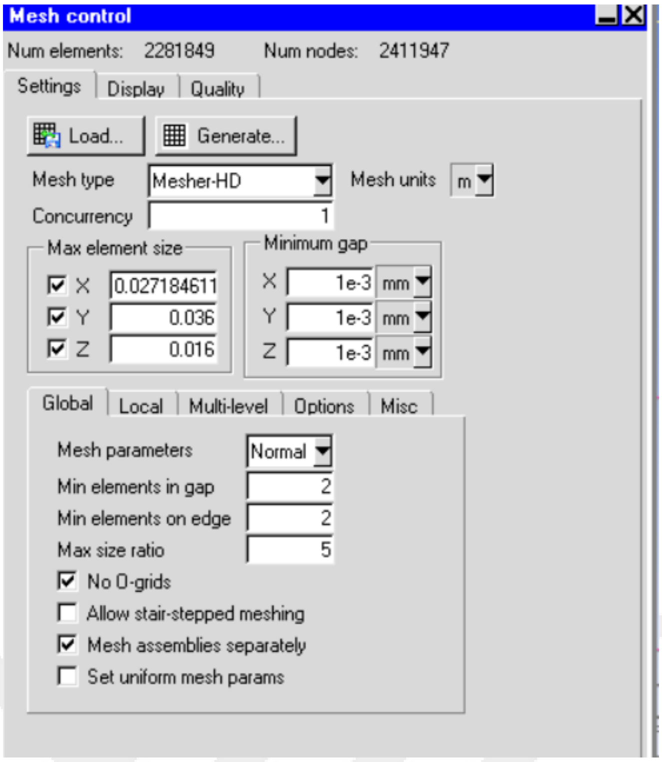

Figure 37: Mesh control for the case of 4014 lateral LED

To optimize the elements, the simulations for different mesh parameters such as maximum element size, minimum number of elements in gap and maximum size ratio are performed to reach the saturation of the junction temperatures in Figure 39. As a result, 2281849 elements and 2411947 nodes in Figure 37 for the case of 4014 LED are determined, for the case of 2010 LED 2158262 elements and 2281764 nodes in Figure 38 are selected to save the simulation time and generating conformal mesh for the simulation.

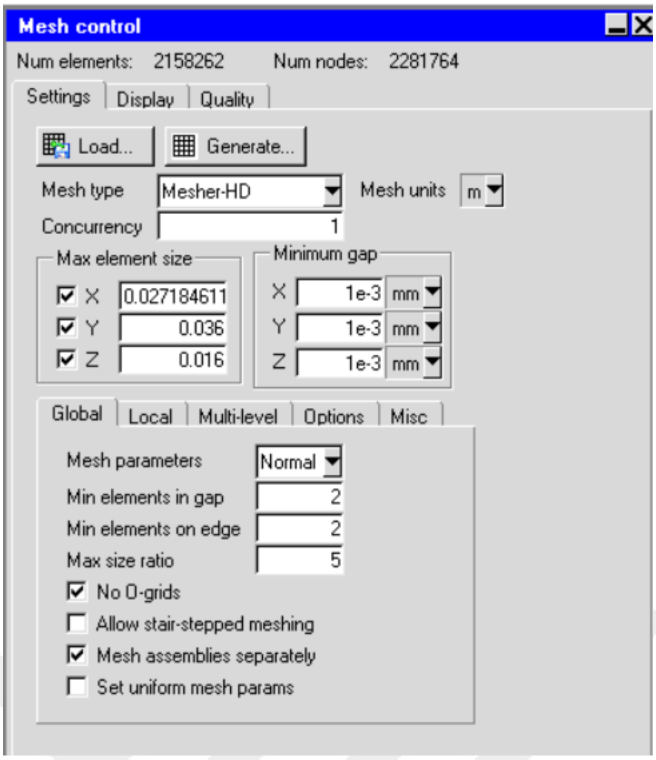

Figure 38: General mesh control for the case of 2010 CSP LED

To reach fine mesh for low volume inner structure of TV is very challenging. As mentioned in the previous sections the component locations inside BLU is very close to each other and it causes some meshing problem such as mesh uniformity and skewness. Mesh uniformity can be defined the cell volume variations from the maximum to the minimum value and the skewness is expressed as an asymmetry between the intersections of the cells. However, the fine mesh generation in Figure 40 is achieved after completing the mesh sensitivity study.

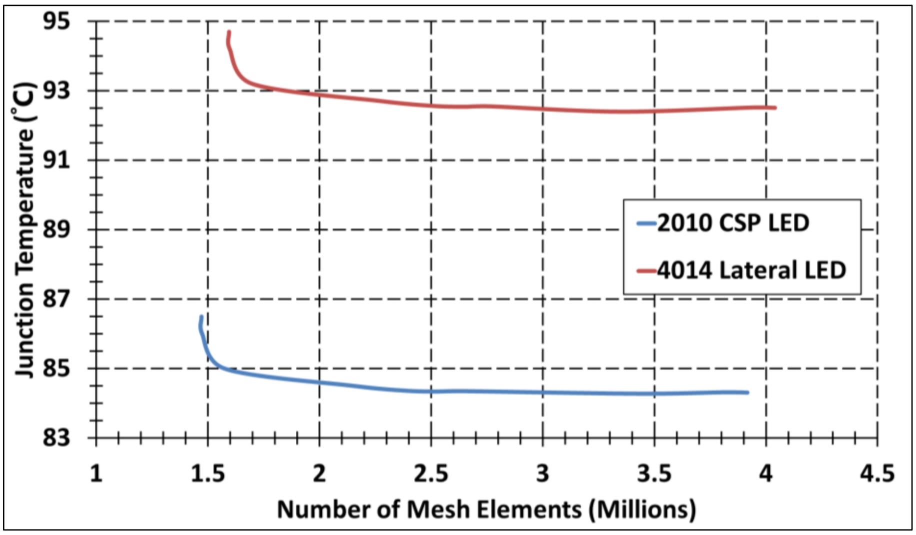

Figure 39: Mesh sensitivity analysis for 4014 and 2010 LEDs

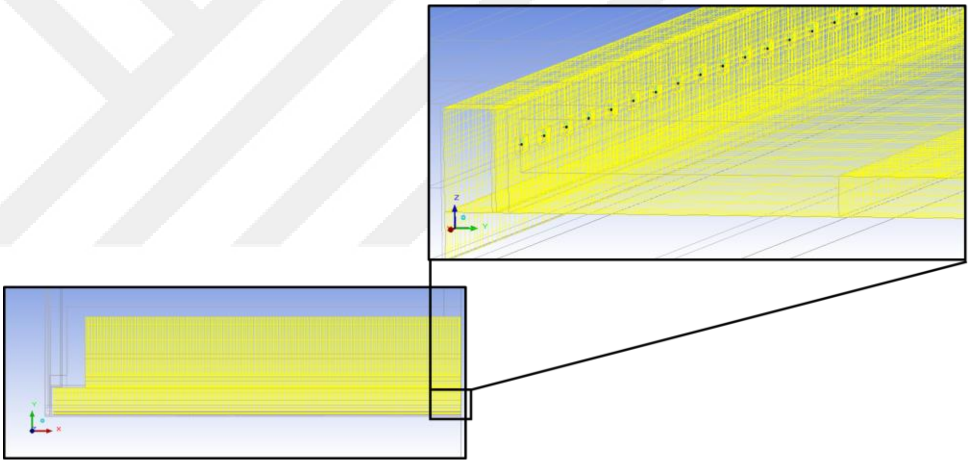

Figure 40: Fine mesh structure on the heat sink

After building the simulation domain, some assumptions are set before executing the simulation. One of them is to select boussinesq approximation since this approach ignores the density difference and is compatible with natural convection problems such as the study. The flow regime is defined as the turbulent due to the inner geometry of the TV. Finally, the simulations are run at 40 °C ambient temperature until steady-state.

4.2.4 Simulation Results

The simulation firstly calculates the Prandtl (Pr) and the Rayleigh (Ra) numbers as 0.708 and 2.3598x10^9, respectively. These dimensionless numbers are used to understand the flow regime. For examples, small values of the Pr, which is Pr << 1, shows that the thermal diffusivity dominate the flow regime. It means that the heat conduction is more important in the system compared to convection. The Rayleigh number is associated with natural convection problem in fluid dynamics, it defines the flow behavior as laminar or turbulent. High value of the Ra such as 10^9 offers the turbulent flow in the system. However, the main purpose of the study to determine the junction temperatures, the temperature distribution on LCD surface and the streamlines into the plastic back cover. The junction temperatures (named network temperatures in simulation) are observed to understand the steady-state during the simulation. The simulation is iterated 900 times to reach the steady-state as presented in Figure 41.

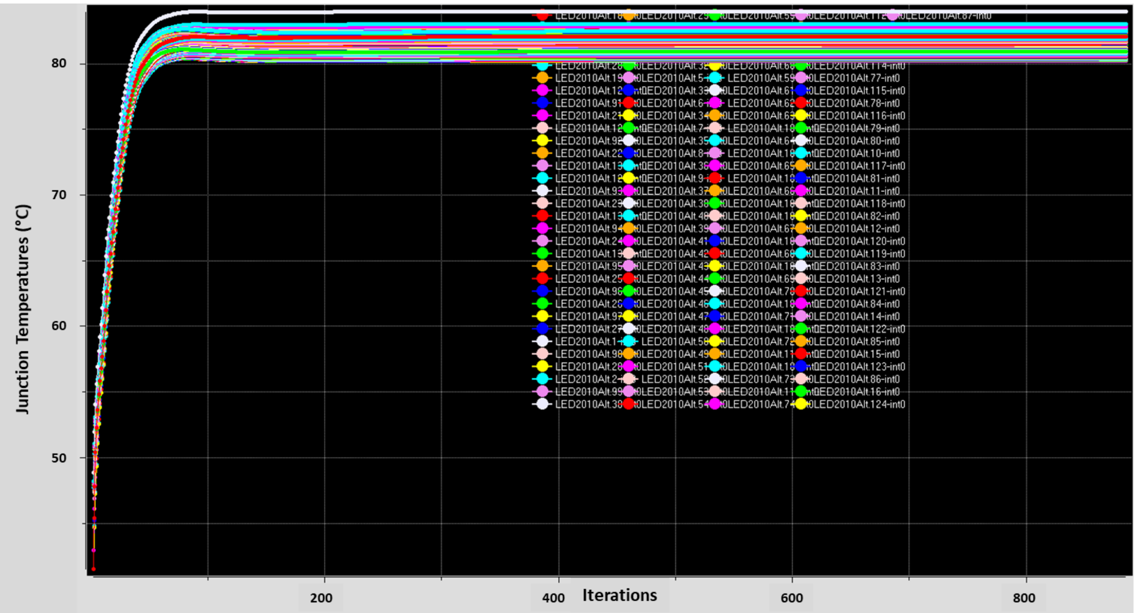

Figure 41: Variation of the junction temperatures with the number of iterations during the simulation

4.2.4.1 Junction Temperatures of LEDs

The average junction temperatures for 4014 lateral and 2010 CSP LEDs are computed as 92.7 °C and 84.5 °C, respectively. The temperature distribution along the LED bar can be seen in Figure 42. According to the graph in Figure 42, the temperature variation along the LED bar is very low such as about ±3 °C for the both case and the lowest temperatures are seen in the middle of the LED bar. For the case of 4014 lateral LED, the junction temperatures exceed the operating value in Table 4 so it causes the decrease of the product life time and some thermal defects on the components. Additionally, low thermal resistance of 2010 CSP LED keeps the junction temperature at low value as a result of the simulation.

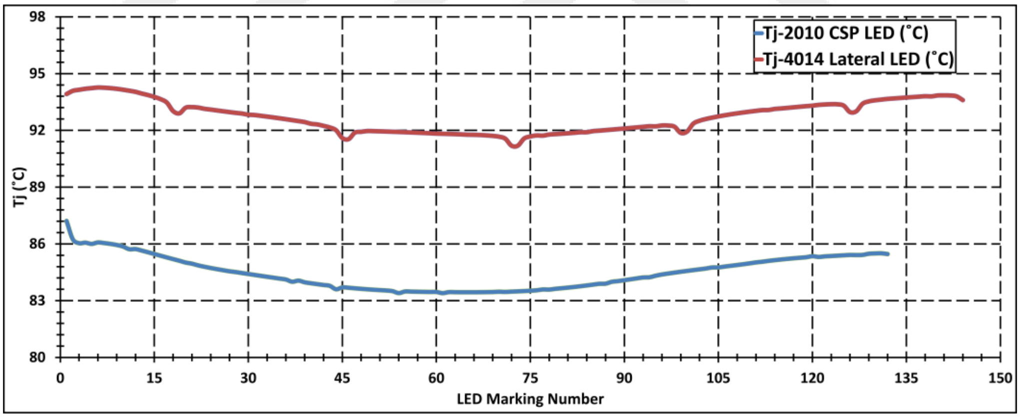

Figure 42: LED junction temperatures

The most effective component on the junction temperature distribution is detected as the component of the heat sink as presented in Figure 43. The temperature contours are similar to the trend of the temperature distribution on the LED bar.

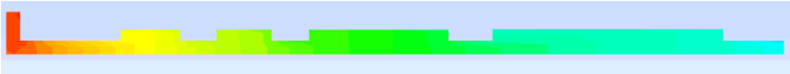

(a)

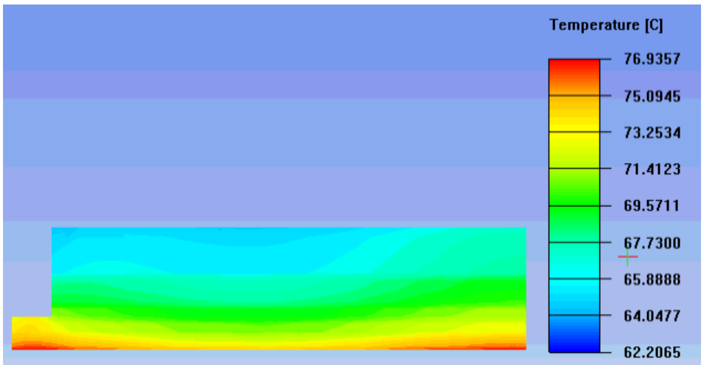

(b)

Figure 43: Heat sink temperature distribution, (a) side view, (b) front view

4.2.4.2 Temperature Distribution on the LCD Surface

The temperature distribution on LCD in Figure 44. The location of the maximum temperature is at the LED bar side and the value is about 61 °C. It is under the absolute maximum in Table 3, so there will be no possible thermal defect on LCD with 112W heat flux. The local hot spots are not seen on LCD due to the uniform heat dissipation on LCD. The reason of the uniform dissipation is the air gap between LCD and BLU structures, the middle frame separates these structures to each other. However, the local hot spots will be significant on BLU optics owing to the interconnection between the heat sink and the optics.

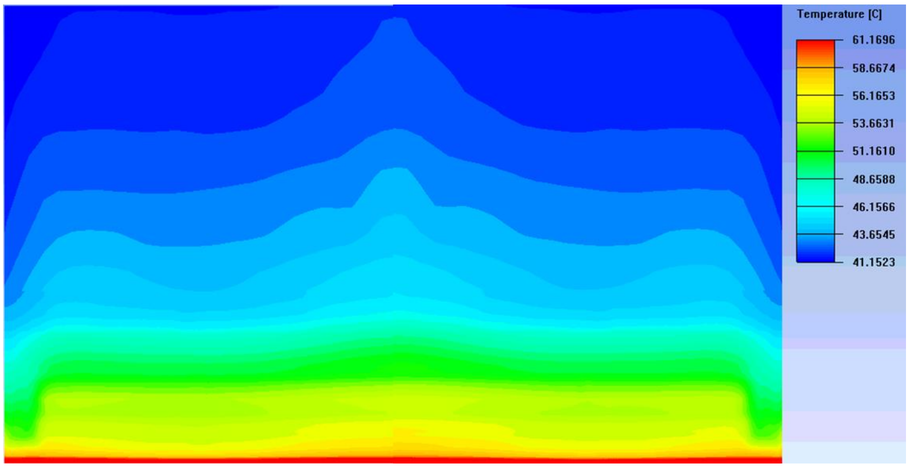

Figure 44: Temperature distribution on LCD surface

4.2.4.3 The Streamlines over the Plastic Back Cover

There is no streamlines inside the BLU due to the tight design but the streamlines is only occurred inside the plastic back cover, where is the volume between the plastic back cover and the metal back cover in the TV. The streamlines in Figure 45 remove the heat from the surface of the metal back cover by convection heat transfer. The Figure 45 shows both of the temperature distribution on the back metal and the streamlines simultaneously. The effect of the streamlines on the temperature distribution can be also seen in the Figure 45.

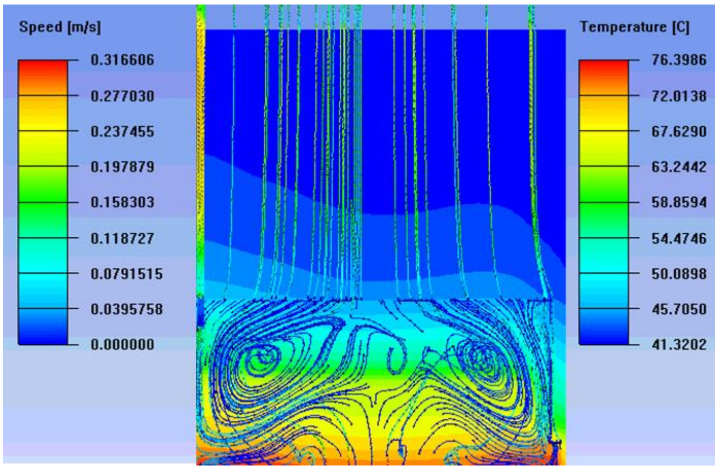

Figure 45: The streamlines on the back side of the metal back cover

The grills on the plastic back cover in the Figure 46 affect the temperature on the metal back cover. The temperatures near the grills are consistently decreased and the influence is transferred to the heat sink from the back metal as well as the junction temperatures. Hence, the design and the placement of the grills are effective on the temperatures of the junction and the whole structure.

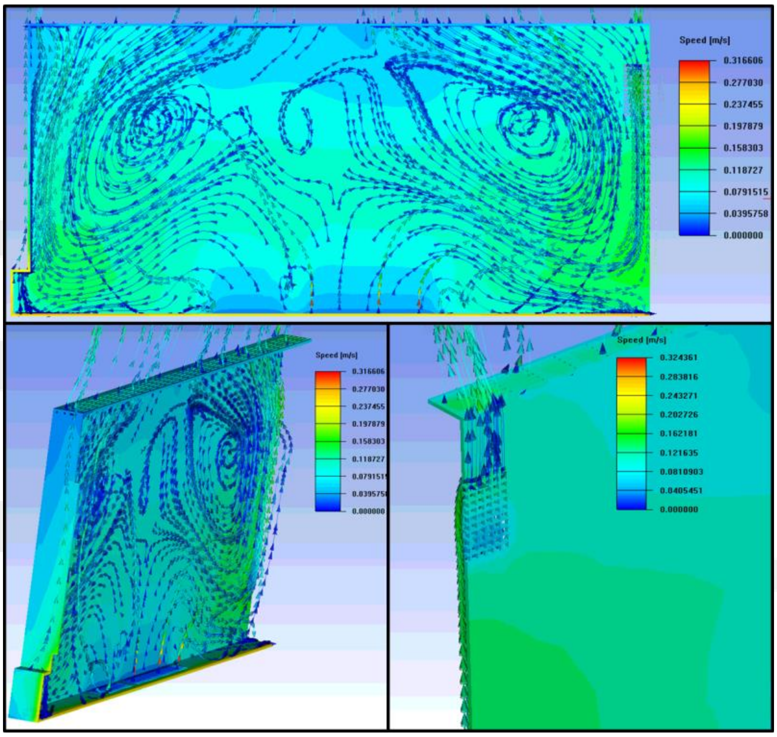

Figure 46: The streamlines inside the plastic back cover and the grills on the plastic BC

CHAPTER V

EXPERIMENTAL STUDY

The thermal and optical behaviors of the 65 inch LED TV are experimentally studied. The aim of the thermal measurements is to validate the simulation results extracted from analytical and CFD models. The second is to compare the temperature distribution on LCD surface with the simulation. The operating and the maximum values of the components such as the LED junction temperature and the surface temperature of LCD are checked if they meet the specifications. In the part of the optical experiments, the optical targets in Table 1 such as center luminance and color gamut of the LED TV are controlled if they are achieved for the case of 140W electrical power.

5.1 Thermal Experiments

Thermal experiments comprise both thermocouple measurements with data logger to reach the junction temperatures and infrared camera (IR) to see the temperature distribution on the LCD. There is no any method to directly measure the LED junction temperature in literature so LED junction temperatures are calculated by utilizing Equation 5. In this method, the solder temperatures (T_s) of LEDs are measured by thermocouples and the junction value are found with Equation. P_{LED} is also electrical input power of LEDs and R_{LED} is the thermal resistance of LEDs. The thermal resistance strongly depends on the LED chip architecture, thus there are two different thermal resistances due to the usage of different type of chip for the study. The first one is the lateral chip. The thermal resistance of the lateral chip is 25 K/W and defined from the solder point to the junction. The second one is the CSP chip, which has novel chip design.

The thermal resistance of the CSP chip is 13 K/W and determined 3 mm away from the junction. CSP LEDs are totally covered by phosphor and resin mixture, so there is no open solder point around the LEDs and having two different thermal resistances. Within the study, the thermal resistance, which is 2 K/W, for junction to base of CSP LEDs is utilized for the thermal models but the thermal resistance 3 mm away from the junction is used for the thermocouple measurements.

$$T_{junction} = T_s + R_{LED}.P_{LED} \quad (5)$$

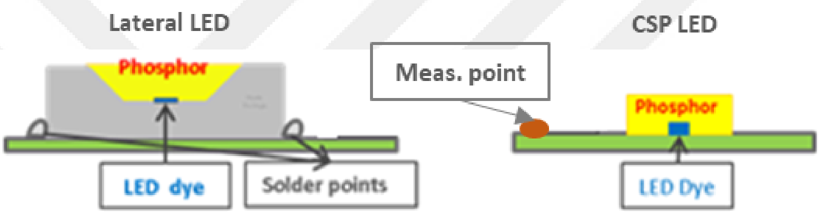

Figure 47: Thermocouple measurement points for LEDs [6]

The thermocouple measurements, which has the accuracy ±2.2 °C, began with making connections the K-type thermocouples and the specific points, which are the solder for the lateral chip and the 3 mm away from the junction for the CSP chip, by using a thermal adhesive material. The measurement points are illustrated in Figure 47. After the measurements, the junction temperatures are calculated by Equation 5. P_{LED} and R_{LED} values are presented in Table 4 as well.

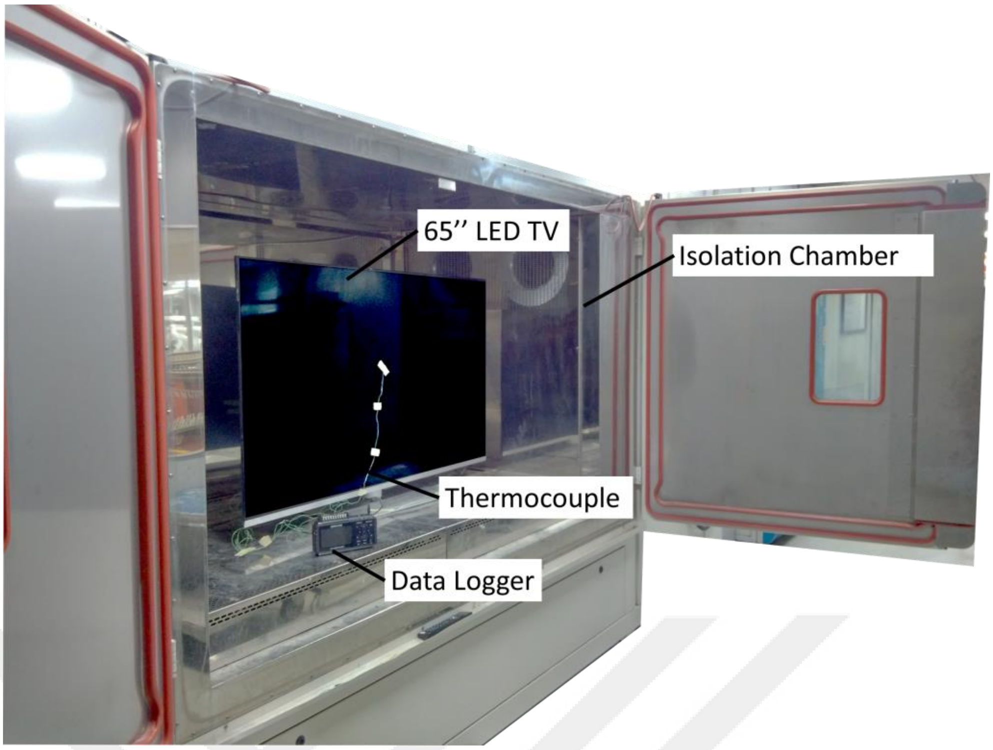

Figure 48: Experimental setup for the thermal test inside the isolation chamber [6]

After bounding the thermocouple to the specific points, the LED TVs are assembled and placed to the isolation chamber in Figure 48. The ambient temperature of the isolation chamber is arranged to 40 °C and then the tests are performed until the steady-state, which can be seen in Figure 49. The thermal data is recorded during 130min to reach the steady-state by Graphtec midi GL220 data logger, which the accuracy is ±1 °C. The results of the thermocouple measurements for the lateral LEDs and the CSP LEDs are presented in Table 7 and the Table 8, respectively.

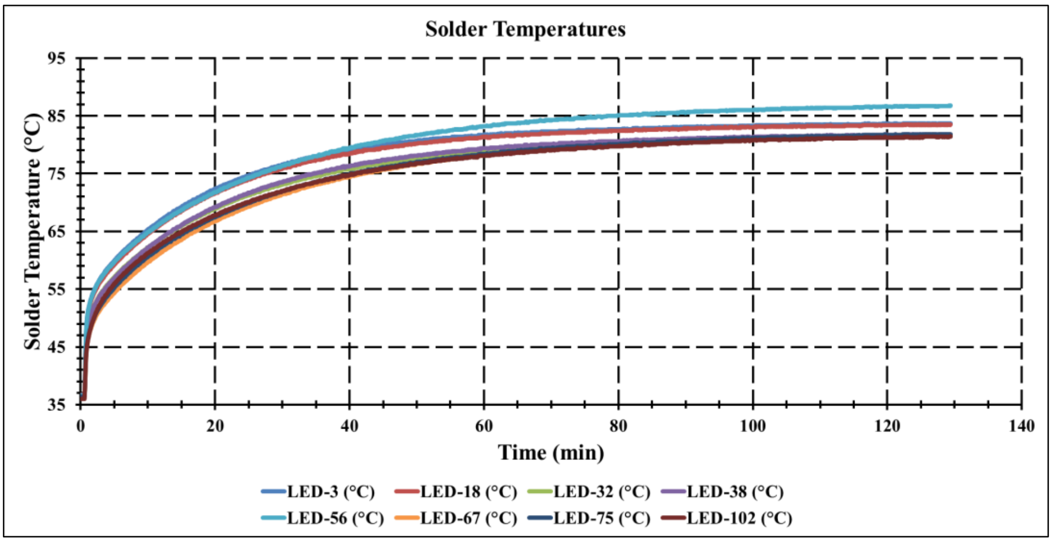

Figure 49: LED solder temperatures during the test

Table 7: The junction and the solder temperatures of lateral LED [6]

Lateral LED	Case to Junction (˚C)	T_{solder} (˚C)	$T_{junction}$ (˚C)
LED-2	11.9	82.7	94.6
LED-22	11.9	82.5	94.4
LED-37	11.9	80.7	92.6
LED-42	11.9	80.8	92.7
LED-64	11.9	85.8	97.7
LED-73	11.9	80.7	92.6
LED-88	11.9	80.8	92.7
LED-114	11.9	80.4	92.3

Table 8: The junction and the solder temperatures of CSP LED [6]

CSP LED	Case to Junction (˚C)	T_{solder} (˚C)	$T_{junction}$ (˚C)
LED-3	6.8	83.2	90.0
LED-18	6.8	80.9	87.7
LED-32	6.8	82.0	88.8
LED-38	6.8	83.9	90.7
LED-56	6.8	85.4	92.2
LED-67	6.8	81.4	88.2
LED-75	6.8	83.7	90.5
LED-102	6.8	82.6	89.4

The results of the thermocouple measurements show that the average junction temperatures for lateral and CSP LEDs are 93.7 °C and 89.7 °C, respectively. The T_j of lateral LEDs is found 4 °C higher than the T_j of CSP LEDs, so CSP LEDs indicates better thermal performance in the TV systems. Furthermore, lateral LEDs do not meet the operating value (88 °C) as presented in Table 4. Therefore, the luminance degradation and the thermal issue is highly possible for the case of the usage of 4014 lateral LEDs. In contrast to the usage of lateral LEDs, CSP LEDs offer long product lifetime and reliability by considering the measurement results since the measured T_j of CSP LEDs is far away from the CSP LED operating value, which is 116 °C.

The other objective of the measurements is to determine the variation between the experiments and the simulations. The calculated variations are presented in Table 9. As expected, the high variation values are found for the analytical models, the main reason of the values is to assume one dimension heat transfer within the analytical model. To reach more accurate result, the heat transfer should be considered in three dimension such as CFD model. The variation of the CFD model is lower due to the assumptions. The mechanical simplification can causes the increase of two variations but it should be made to reach a fine mesh generation.

As a second part of the experiments, IR camera measurements are taken from the surface of the LCD. The aim of the measurement is to see the temperature distribution on the surface. Before the measurements, the correlation factor is defined between the thermocouple and IR camera measurements. The reference thermocouple is bounded on the surface of the LCD during the test. Then, the emissivity value of the glass surface is arranged to 0.95 in the settings of the IR camera. The thermal images are taken at 40 °C ambient by Fluke Ti125 thermal camera, which has the accuracy of ±2 °C, after the system reaches the steady-state. The images taken by IR camera for the cases f 4014 lateral and the CSP LEDs can be seen in Figure 50 and Figure 51, respectively.

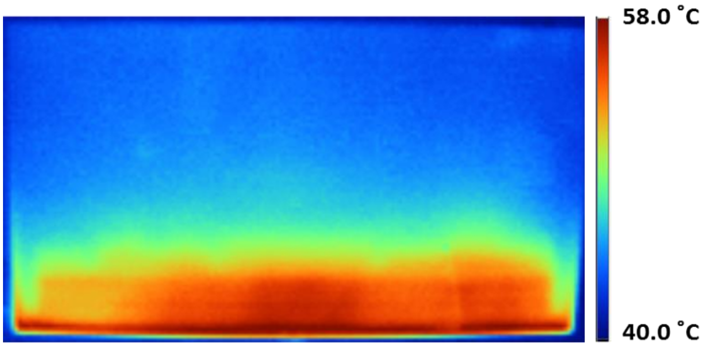

Figure 50: The IR image of the LCD surface for the case of 4014 lateral LED [6]

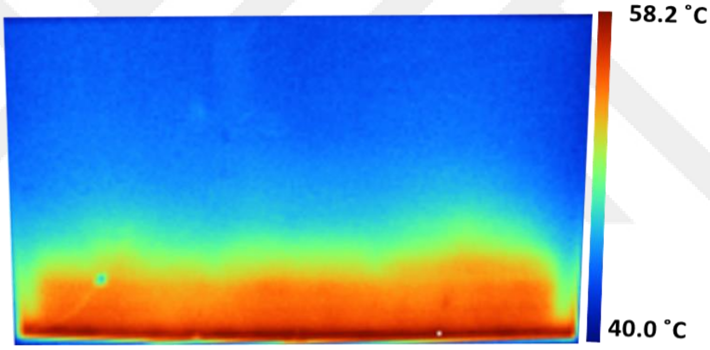

Figure 51: The IR image of the LCD surface for the case of CSP LED [6]

The temperature distribution in Figure 50 and Figure 52 seems to be similar for two cases since the components except LEDs are same in the system. Due to the assumption of the same heat flux generation for two cases, the heat dissipation should be similar along the LCD. It is clearly seen that the heat sink remove the heat from the system when looking at the images. Some amount of the heat generation is directly transferred to the LCD owing to the interconnection surfaces between the heat sink and the optics. The temperature distribution for both the simulations and the IR images are presented in

Figure 52. The temperature values in Figure 52 are extracted from the middle line of the LCD, which is illustrated on the graph in the Figure.

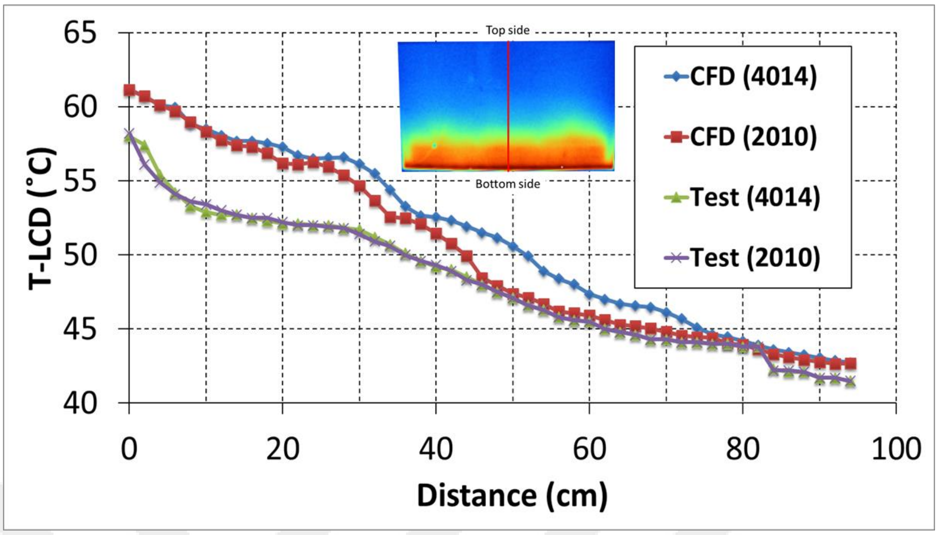

Figure 52: Temperature distributions from the bottom side to the top side of the LCD

According to the graph in Figure 52, the trend lines regarding to the distribution near the LED bar for the IR images have more smooth transitions but the simulation trend lines around the LED bar behave linearly or having sharp transitions. The root cause of the issue can be sourced of some assumptions regarding to LCD structure in simulation domain because the LCD structure in simulation is simply created with rectangular objects. However, there are complex layers in a real LCD structure. The LCD inner structures are consisted of thin film transistors (TFT) and different layers such as color filters and polarizers, so it causes to assume a common thermal resistance of the whole LCD layers. Likewise, the LCD in simulation domain is assumed to only one layer in the simulation domain. Therefore, it can increase the variations for the temperature distribution on the LCD for the simulation case.

Table 9: T_j values and the variations between experimental and numerical results

Items	4014 Lateral LED	2010 CSP LED
$T_{j\text{-sim\_analytical}}$ (˚C)	84.2	75.3
$T_{j\text{-CFD}}$ (˚C)	92.7	84.5
$T_{j\text{-measured}}$ (˚C)	93.7	89.7
Analytical variation (%)	10.1	16.0
CFD variation (%)	1.2	5.8

Table 10: Uncertainty analysis for the junction temperature [22]

No.	Items	Error (°C)	Systematic uncertainty (°C)	Random uncertainty (°C)	Total uncertainty (°C)	Expanded uncertainty (k=2) (°C)
1	**Data logger**	± 1	2.42	2	3.12	6.24
2	**Thermocouple**	± 2.2				
Standard Deviation		± 2.0°C				

5.2 Optical Experiments

The optical specifications of TV are checked by taking optical measurements within this study. As stated before, there are two BLU cases composed of 288pcs 4014 lateral LEDs and 264pcs 2010 CSP LEDs. Lateral LEDs are driven 81mA and 5.9V, and also the driving current and forward voltage of CSP LEDs are 175mA and 3.0V, respectively. These values are determined by considering the power board constraints, which the maximum power consumption is 140W. The optical targets such as center luminance and color gamut particularly depend on the lumen output of the light source and the spectral characteristics. The optical measurements are taken by using the standard test setup presented in Figure 53. According to the setup, the spectroradiometer (with 2% accuracy) is located 50 cm away from the TV and the TV is kept on vertical position against the spectroradiometer. Before the measurements, the fully white content meaning the open condition of all pixels is arranged as an image in TV settings and the spectral power distribution (SPD) measurements are taken at the center of the LED TV. The measurements are repeated for red, green and blue images meaning the open condition of each sub pixel separately to calculate the color gamut.

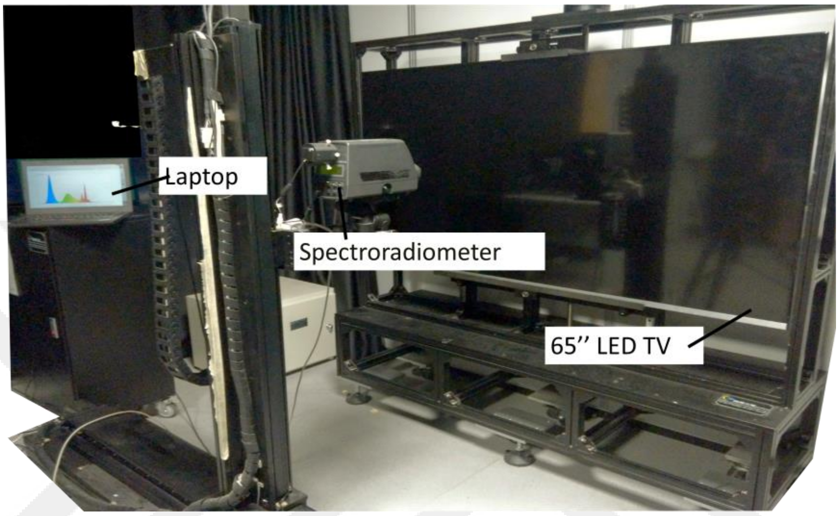

Figure 53: Standard optical test setup [6]

The values of SPD are used to calculate the center luminance and the color gamut of the LED TV. Then, the results are presented in Table 10. According to the measurements, CSP LEDs offer 20% higher luminance compared to lateral LEDs under the same power consumption. The luminance difference between two cases can be seen when compared to the spectrums in Figure 54. The other issue is that the 4014 lateral LEDs can not meet the center luminance requirements of the TV. The driving current of 4014 LEDs should be increased by an amount of 25% to reach the luminance target, but the level of the junction temperatures with an existing current value 81mA are above the limit value. Hence, the increase of the driving current causes the higher temperatures than the operating values. Likewise, the low product lifetime and the thermal issue will be highly possible. For the case of CSP LEDs, the LED TV with higher luminance is possible due to the margin of the driving current.

Table 11: Center luminance and color gamut values of the LED TV [6]

LED Array Type	Center luminance(nit)		Color Gamut in CIE 1976 (%)
	TV	BLU	
4014 Lateral LED Case	398.2	7554	90
2010 CSP LED Case	502.1	9556	92

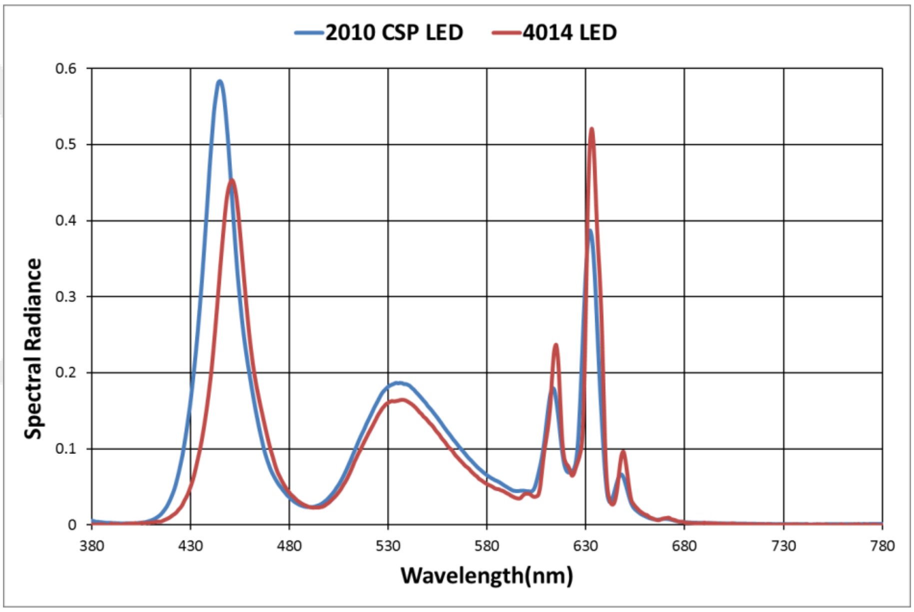

Figure 54: SPD of the BLUs with 4014 lateral and 2010 CSP LED [6]

Regarding to the color gamut, it depends on the spectral characteristic of the light source, but the shape of the spectrum is changed due to the thermal stress if the junction temperatures exceed operating values. Within the study, the junction temperature of 4014 lateral LEDs can not provide the operating value, so the color gamut value of the case of 4014 lateral LED is found 2% lower than the case of 2010 CSP LEDs, which is given in Table 10. The color gamut is getting lower if the driving current is increased to reach the center luminance target for the case of 4014 LEDs. It is the proof of the thermal effect on the color gamut as well.

Table 12: Uncertainty analysis for the center luminance [22]

No.	Items	Error (nit)	Systematic uncertainty (nit)	Random uncertainty (nit)	Total uncertainty (nit)	Expanded uncertainty (k=2) (nit)
1	**Spectroradiometer**	± 8	40.6	10	41.8	83.6
2	**BLU components**	± 39.8				
Standard Deviation		± 10 nit				

CHAPTER VI

SUMMARY AND CONCLUSIONS

The main purpose of this study is to determine the optimal LED type for a 65-inch ultra-thin LED TV by creating thermal models and considering the optical gain of the light source. In the recent years, some challenging optical requirements such as high brightness and wide color gamut with an ultra-thin TV structure are demanded in the high-end TV market. To meet the targets, the TV makers need to consider thermal efficiency and optical gain in parallel during the design stage. At present, the usage of the LEDs doped with KSF phosphor in BLU design is the key point instead of the thermal sensitivity of KSF material. Within the study, various LED chip types covered by KSF phosphor are investigated in a 65-inch LED TV by utilizing the thermal models such as analytical and CFD and performing the standard optical tests on the LED TV. The junction temperatures of LEDs are crucial factor to validate the thermal models with the experiments and figure out the product lifetime. The variations of the CFD model for lateral and CSP chips are found 1.2% and 5.8%, respectively. However, high variations in Table 9 for the analytical models seem due to the assumption of the one dimension heat transfer. The other finding is the temperature distribution on the LCD surface. The temperature distributions on the LCD in Figure 52 shows some inconsistencies between the experimental and the numerical results. The assumptions of the LCD in simulation domain cause the increase of the variations. In particular, the complex inner structures of the LCD is the main reason of the high variation. Additionally, the CFD model is an occasion to see the streamlines effect inside the plastic back cover on the component temperatures. There is no another way to observe this effect in a real life. As far as the optical performance is concerned, the optical targets are checked for two cases such as lateral and CSP LEDs and then the

25% higher luminance for the case of CSP LEDs is measured by the standard test setup. Hence, CSP LEDs seem to be the best choice to meet the requirements of the high-end TVs. On the other hand, the case of lateral LEDs is still used for the solution of the LED TV with lower brightness as well. For now, CSP LED solution can be evaluated in the high-end TV market but it is inconvenient solution for use in the standard TV markets due to the high cost of the manufacturing process. In the future, the inner structure of the LCD such as polarizers, color filters and TFT structure might be added in the simulation domain to investigate more accurately the temperature distribution on the surface. And also, the simulation may include the COF IC of the LCD. The other one might be to directly use the complex geometry without any mechanical simplifications in the simulations. Finally, the multi-physics simulations including thermal and optical parameters for a LED TV might be created to investigate thermal efficiency and optical gain of the system at the same simulation domain.

BIBLIOGRAPHY

[1] IHS Markit, 2018, “TV Display Market and New Technology – LCD, OLED, QLED, Micro LED TV”, [PowerPoint Slides] available at: <http://xqdoc.imedao.com/16184d36f5150de13fd3f231.pdf > [Accessed 02 June 2019]

[2] HIS Technology, 2016, “Wide color gamut market tracker 2016”, [PowerPoint Slides] available at: <https://cdn.ihs.com/www/pdf/1118/abstract-wide-color-gamut-market-tracker.pdf> [Accessed 02 June 2019]

[3] Wikipedia, 2009, “CIE 1931 color space chromaticity diagram”, [Online] available at: https://en.wikipedia.org/wiki/CIE_1931_color_space [Accessed 03 June 2019]

[4] L. Wang, X. Wang, T. Kohsei, K. Yoshimura, M. Izumi, N. Hirosaki and R. J. Xie, “Highly efficient narrow-band green and red phosphors enabling wider color gamut LED backlight for more brilliant displays”, Optical Society of America (DOI:10.1364/OE.23.028707), 2015

[5] www.energy.gov, 2018, “Narrow-Band Emitting Phosphors for Energy Efficient SSL”, [PowerPoint Presentation] available at: < https://www.energy.gov/sites/prod/files/ 2018/02/f49/murphy_phosphors_nashville18.pdf> [Accessed 08 June 2019]

[6] M. Elibol, M. Ç. Özaydın and M. Arık, “Development of a Computational Modeling and Experimental Validation Approach for KSF LED Packages in a 65” Ultra-Thin LED TV System”, 17th IEEE ITHERM Conference (978-1-5386-1272-9), San Diego, 2018

[7] J. Fan, C. Qian, M. Zhang, Y. Li, X. Fan and G. Shang, “Thermal, Optical and Electrical Analysis on Phosphor-converted White LED Chip Scale Packages with Both Experiment and Simulation”, 17th International Conference on Thermal, Mechanical and Multi-Physics Simulation and Experiments in Microelectronics and Microsystems (978-1-5090-2106-2/16), 2016

[8] Y. K. Chen, M H. Lin and K. F. Huang, “Analysis for LED Junction Temperature in LCD Module Based on Numerical Simulation”, SID 08 DIGEST (008-0966X/08/3903-1629), 2008

[9] C. C. Huang, H. L. Yang and A. Tzeng, “Edge-Type LED Module Mura Analysis and Improvement”, SID 11 DIGEST (0097-966X/11/4202-0758), 2011

[10] A. Konno, M. Abe, Y. Aono, K. Nakamura, M. Tsumura and I. Hiyama, “Ultra-Thin IPS-pro LCD-TVs Using Simple Side-Edge Backlight with RGB-LED and Novel Heat Radiation Structure”, SID 09 DIGEST (009-0966X/09/3902-0716), 2009

[11] Y. C. Tsai and Y. W. Chen, “Cooling Efficiency Improvement of LCD Module by High Emissivity Surface Treating in Natural Convection Condition”, SID 08 DIGEST (008-0966X/08/3903-1598), 2008

[12] H. L. Yang, Y. W. Chen and Alex Tzeng, “Improvement of Thermal Uniformity of LED Backlight Module by Irregular Bracket Design”, SID 09 DIGEST (009-0966X/09/3902-0830), 2009

[13] C. Y. Chu and M. C. Pan, “Effective thermal emission on TFT–LCD TV panels for improving image quality”, Advances in Engineering Software (0965-9978), 2009

[14] M. İz, İ. Tavman and A. Turgut, “A Study on Cooling Efficiency Improvement of Thin Film Transistor Liquid Crystal Display (TFT-LCD) Modules”, 13th Electronics Packaging Technology Conference (978-1-4577-1982-0/11), 2011

[15] Wikipedia, 2009, LCD RGB sub pixel. [online] Available at: <http://pl.wikipedia.org/wiki/Plik:LCD_RGB_subpixel.jpg> [Accessed 13 June 2019]

[16] J. Li and G. Q. Zhang, The TEX Book, Reading, “Light-Emitting Diodes: Materials, Processes, Devices and Applications”, Reprinted as Vol. 4 of Solid State Lighting Technology and Application, 2018

[17] O. R. Adetunji, “Optimizing Hot Dip Galvanizing Operations Of Steel Sheets For Better Quality”, Journal of Natural Science Engineering and Technology (9(2):99-105), 2010

[18] K. Karslı, Thesis, “Development of Various Corner-lit Backlighting Concepts in an Advanced Smart Led TV”, 2015

[19] www.shinwha.com, 2017, “Smart Optical Film – Multi Sheet ”,
[online] Available at:
< http://www.shinwha.com/eng/web_html/product/product01.php >
[Accessed 01 August 2019]

[20] www.shinwha.com, 2017, “Smart Optical Film - Single Sheet”,
[online] Available at:
<http://www.shinwha.com/eng/web_html/product/product02_tab04.php>
[Accessed 01 August 2019]

[21] www.shinwha.com, 2017, “Smart Optical Film - Single Sheet”,

[online] Available at:

<http://www.shinwha.com/eng/web_html/product/product02_tab03.php>

[Accessed 01 August 2019]

[22] A. Prasad, Thesis, “A Detailed Uncertainty Analysis of Heat Transfer Experiments Using Temperature Sensitivity Paint”, 2016

APPENDIX 1

A. Formulas for Uncertainty Analysis

There are two types of uncertainty, these are systematic and random error. The sum of both uncertainty is named as the total uncertainty.

Systematic Uncertainty

This uncertainty is calculated from the bias error of the measurements taken from a measuring device. It is the same for a single test and uses the root sum square method to define the errors in the measurement. It is present in equation 6,

$$B_{\bar{x}} = \sqrt{e_1^2 + \ e_2^2 \ \dots \dots + e_n^2} \tag{6}$$

In this equation, e_1, e_2..... e_n are the different types of errors in a measuring device for a single measurement.

Random Uncertainty

The repeatability of the experiment offers random uncertainty. The standard deviation is utilized to calculate random uncertainty.

$$B_{\bar{x}} = \frac{\sigma_x}{\sqrt{N}} \tag{7}$$

In the equation 7, σ_x is the standard deviation of the recorded measurement and N is the number of measurement.

Total Uncertainty

It is the combination of systematic and random uncertainty, with the utilization of root sum square method.

$$u_{\bar{x}} = \sqrt{B_{\bar{x}}^2 + S_{\bar{x}}^2} \tag{8}$$

VITA

Metehan Elibol obtained his Bachelor's Degree from the Department of Physics Engineering at Hacettepe University. He completed master programme of Mechanical Engineering at Ozyegin University. His research interests are the optical design of opto-mechanical systems and the thermal management of LED TVs. He specifically has experience to design the optical part of backlight systems in LED LCD TVs. He currently works for Vestel Electronic Company as optical system design architect.